

A NEW SET OF TOOLS FOR GOODNESS-OF-FIT VALIDATION

GILLES R. DUCHARME AND TERESA LEDWINA

ABSTRACT. We introduce two new tools to assess the validity of statistical distributions. These tools are based on components derived from a new statistical quantity, the *comparison curve*. The first tool is a graphical representation of these components on a *bar plot* (B plot), which can provide a detailed appraisal of the validity of the statistical model, in particular when supplemented by acceptance regions related to the model. The knowledge gained from this representation can sometimes suggest an existing *goodness-of-fit test* to supplement this visual assessment with a control of the type I error. Otherwise, an adaptive test may be preferable and the second tool is the combination of these components to produce a powerful χ^2 -type *goodness-of-fit test*. Because the number of these components can be large, we introduce a new selection rule to decide, in a data driven fashion, on their proper number to take into consideration. In a simulation, our goodness-of-fit tests are seen to be power-wise competitive with the best solutions that have been recommended in the context of a fully specified model as well as when some parameters must be estimated. Practical examples show how to use these tools to derive principled information about where the model departs from the data.

CONTENTS

1. Introduction	2
2. The case of a simple null hypothesis	4
2.1. The comparison curve (CC)	4
2.2. Nested partition of $(0,1)$ and projected Haar functions $\{h_{s,j}(\cdot)\}$	6
2.3. Fourier coefficients of the comparison density in the system $\{h_{s,j}(\cdot)\}$	6
2.4. χ^2 -type test statistic and selection rule for its number of components $d(s)$	7
2.5. A simulation experiment	8
3. Composite null hypothesis	10
3.1. Fourier coefficients and empirical CC	10
3.2. CC and alternatives in the case of location-scale models	11
3.3. The bar plot (B plot) in the composite and simple null cases	11
3.4. χ^2 -type test statistic and a selection rule for $d(s)$ for testing Gaussianity	12
3.5. A real data example: wave records	14
4. Discussion	15
References for Sections 1 to 4	16
Appendix A. Real data examples	18
A.1. The wave record data revisited	18
A.2. The open/closed book examination data	21
A.3. The cystine data	22
A.4. The tephra data	23
A.5. The PCB data	24
A.6. The smiling baby data set revisited	25
Appendix B. Details and recommendations on the implementation of our tools	26
Appendix C. The simulation experiment for a composite Gaussian null hypothesis and related comments	28
Appendix D. Proofs	31
D.1. Proof of Proposition 1	31
D.2. Proof of Proposition 2	32
D.3. Proof of Remark 1	34
References for Appendices	34

Key words and phrases. Chi-square test; Comparison curve; Data driven test; Diagnostic component; Graphical inference; Model validation; Selection rule; Smooth test.

1. INTRODUCTION

Let X be a random variable with unknown cumulative distribution function (CDF) $F(\cdot)$. Statistical models are entertained approximations to $F(\cdot)$ which serve to produce inferential statements about the behaviour of X . Constructing a good approximation is an iterative process where at any given step, a contemplated model based on previously acquired knowledge, external considerations, etc., is assessed by confrontation with data. When the current proposal is invalidated, its defects must be learned to explore a better model at the next iteration. When a model is tentatively validated, useful inference can be drawn by exploiting its characteristics, allowing the accumulation of subject matter knowledge.

In the present work, the entertained statistical model for X is the CDF $F_0(\cdot; \beta)$ where the parameter β may be unknown. The data is a sample of independent copies X_1, \dots, X_n of X .

Two main routes exist for statistical model validation. A first one focusses on graphical representations, such as PP (percentile-percentile) or QQ (quantile-quantile) plots (Thas, 2010). When the model is valid, these plots should closely follow the 45-degree line through the origin. Deviations can provide insights about where the data do not conform to the entertained model. These visual appreciations can be supplemented with confidence regions about such representations (Aldor-Noiman et al., 2013; Gan et al., 1991) or test statistics measuring departure from this straight line (Gan & Koehler, 1990) to control the type I error (i.e. falsely considering a model is invalid). This route can clearly be a cog in the modelling process.

A second route focusses mainly on error risks by testing, via formal goodness-of-fit (GoF) procedures, the null hypothesis that the model holds. A large number of test statistics have been derived for such problems (for testing the GoF to the Gaussian distribution, Arnastauskaité et al. (2021) list 40 such tests) which allow controlling the type I error risk. Regarding the type II error (i.e. not rejecting an invalid model and thus stopping prematurely the modelling process), an enormous amount of work has been accomplished, both theoretically and empirically, to understand the respective power of the various proposals and to derive a generally good solution for specific problems. In particular, regarding the Gaussian distribution again, a long series of simulation experiments have been conducted (see Arnastauskaité et al. (2021) and references therein) to characterize the effectiveness of popular proposals. A first drawback is that it is not easy to decide, in view of the data at hand, upon an appropriate GoF test among this plethora of solutions. Another drawback is that when the chosen test rejects, the user is often left with little information about the defects of the model. This makes it difficult to pursue the modelling process.

A few exceptions are the well-known Pearson χ^2 -test and the χ^2 -type smooth test introduced by Neyman (1937), to which sets of components can be associated. Each component reacts to specific departures and if these can be discerned, their inspection can help a user gain some insights about where the model is at fault. Below, we discuss some problems arising when β is known. Both approaches have been extended to the case of unknown β but even more serious difficulties occur.

There are two main problems with χ^2 and χ^2 -type tests. The first one arises from the standard order of the argument leading to these components, which is first to get from external considerations a GoF test, then try to extract meaningful components. For Pearson's χ^2 -test, Anderson (1994) has made such an attempt but Boero et al. (2004a) have shown that his approach was not completely successful; for similar efforts, see Voinov (2010) and references therein. Regarding Neyman's smooth tests, meaning depends on the orthogonal system used in the test. With

classical orthogonal polynomials, the first few components will typically be associated with central moments (Thas, 2010), but beyond the third (skewness) they become difficult to relate to telling departures. For the classical Pearson's χ^2 -square test with β known, the components are not easy to interpret as they heavily depend on the selected partition. The second problem concerns the number of components to be used in the test: too few or too many negatively affect the power of the test. For some historical notes and recommendations about choosing the partitions, see Boero et al. (2004b) and Rolke & Gongora (2021). Bogdan (1995) and Inglot & Janic-Wróblewska (2003) contain some useful proposals regarding data driven selections of the partition in classical χ^2 -test. Some data driven GoF tests based on partitions have also been derived in Section 5.5 of Thas (2001). In turn, Ledwina (1994) has proposed an effective way of selecting the number of components in the classical Neyman's smooth test.

In the present work, we try to solve these problems by introducing easily interpretable components, different from those in the original χ^2 -test and several variants of Neyman's test, which can be graphically represented to give a detailed appraisal of the validity of a model. Acceptance regions for subsets of components under the null model can be plotted to sharpen the insight gained from the graphical representation. This may help in selecting an adequate GoF test to assess the global fit between the data and the model. When, likely, none naturally emerges, the components can be combined to produce a new powerful data driven χ^2 -type GoF test supplementing the visual assessment with a control of the type I error.

We start by introducing a function, referred to as the *comparison curve* (CC), which is related to existing statistical objects such as PP plots. Its evaluation yields components whose statistical properties offer richer insights, when represented on what we call a *bar plot* (B plot), than PP or QQ plots. In particular, this first new tool allows to gain some ideas about where (in terms of ranges of quantiles of the model $F_0(\cdot; \beta)$) and to which extent the data contradict the model. These components are then shown to be aggregated successive Fourier coefficients of the *comparison density* (see Section 2.3). This allows formulating the validity of the model as the vanishing of these coefficients. The number of such components can in principle be as large as one chooses. Hence a second important task is to derive a way of selecting, in a data driven fashion, their number. We introduce a new selection rule to decide on a proper number of components to include in our second tool, a *data driven χ^2 -type GoF test statistic*. Finally, we show how the B plot can be supplemented with acceptance regions for subsets of components to provide more precise indications regarding the compatibility of the data with the null model in some regions of interest.

We first consider the context where the null model $F_0(\cdot; \beta)$ is entirely specified, i.e. β is known. A carefully balanced simulation experiment shows that our procedure competes with some best tests in this context. Then we move to the context where the parameter β in $F_0(\cdot; \beta)$ must be estimated. Particular attention is given to the location-scale model, i.e. $F_0((x - \beta_1)/\beta_2)$, and to the important sub-case of a Gaussian model. Again the results of a balanced simulation experiment show our procedure competes with some best tests for this set-up. In both contexts, we apply our tools to real data to show how useful insights can be derived. The appendices contain supplementary information regarding the application of our methods to six data sets, a discussion about how B plots can be used in deciding upon an adequate GoF test to assess the overall fit of data to a postulated model, how to apply them to design well balanced simulation studies, some practical recommendations in using our tools, the results of the simulation experiment comparing our proposal to some best solutions and the proofs of various technical results.

2. THE CASE OF A SIMPLE NULL HYPOTHESIS

2.1. The comparison curve (CC). Let X_1, \dots, X_n be a sample of i.i.d. observations from an unknown continuous CDF $F(\cdot)$. We start by considering the case where the parameter β in the continuous model $F_0(\cdot; \beta)$ is known and write for simplicity $F_0(\cdot)$ for this CDF. The simple null hypothesis of interest is

$$(2.1) \quad \mathbb{H}_0 : F(\cdot) = F_0(\cdot).$$

Consider the random variable $Z = F_0(X)$. By the *probability integral transformation*, when $X \sim F(\cdot)$, Z has CDF $H(p) = F(F_0^{-1}(p))$, $p \in (0, 1)$, which is referred to by Parzen (2004) as the *comparison CDF*, because when some auxiliary random variable $X_0 \sim F_0(\cdot)$, then $H(\cdot)$ is the CDF of X expressed on a scale in which $X_0 \sim U(0, 1)$. $H(\cdot)$ is also referred to in the literature as the *relative distribution* (Handcock & Morris, 1999) as Z measures the relative ranks of X compared to $X_0 \sim F_0(\cdot)$. Such relative ranks are also known as the *grade transformation* following a statistical tradition that goes back to Galton; cf. Kendall & Buckland (1957). The function $H(\cdot)$ is also the population version of the PP plot of $F(\cdot)$ against $F_0(\cdot)$ which, in this context, is sometimes called the reference distribution.

The approach of the present work is based on a standardized version of the *comparison CDF*, which we call the *comparison curve (CC)* and define as

$$(2.2) \quad CC(p) = \frac{p - F(F_0^{-1}(p))}{\sqrt{p(1-p)}}, \quad p \in (0, 1).$$

When \mathbb{H}_0 holds, $CC(\cdot) \equiv 0$ and otherwise captures weighted vertical discrepancies between the population PP plot and the 45-degree line. As with PP plots, $CC(\cdot)$ is invariant under monotone transformations of the measurement scale. But in contrast with PP plots which are always 0 as $p \rightarrow 0$, and 1 as $p \rightarrow 1$, $CC(\cdot)$ can be unbounded at the boundaries, see the Lehmann contamination and the Anderson kurtotic alternatives in Figure 2.2. Due to the meaningful weighting in (2.2), $CC(\cdot)$ can better exhibit differences between $F(\cdot)$ and $F_0(\cdot)$ appearing in tails; see below. Moreover, plots of $CC(\cdot)$ can be interpreted similarly as population PP plots. In particular, if $CC(p) \geq 0$ for all $p \in (0, 1)$, then $F(\cdot)$ is stochastically larger than $F_0(\cdot)$. If there is only one point $p_0 \in (0, 1)$ such that $CC(p_0) = 0$, then $F^{-1}(p_0) = F_0^{-1}(p_0)$ and consequently, the set $(-\infty, F_0^{-1}(p_0)]$ has the same probability under both $F(\cdot)$ and $F_0(\cdot)$. Obviously, the same conclusion holds for the set $(F_0^{-1}(p_0), +\infty)$. The relation $CC(p) > 0$ on $(0, p_0)$ defines the region where $F_0(\cdot) > F(\cdot)$. Hence, when restricted to this interval, observations generated from the conditional distribution of $F(\cdot)$ are stochastically larger than under the respective conditional variant of $F_0(\cdot)$. Otherwise stated, the probability mass associated with $F(\cdot)$ accumulates more intensively toward $F_0^{-1}(p_0)$ than the mass of $F_0(\cdot)$. In terms of quantiles, we get $F_0^{-1}(\cdot) < F^{-1}(\cdot)$ and the quantiles of $F(\cdot)$ are more concentrated toward the p_0 -quantile of the reference CDF $F_0(\cdot)$ than those of $F_0(\cdot)$ itself. The reverse holds when $CC(\cdot) < 0$ on $(0, p_0)$. The magnitude of $CC(\cdot)$ reflects the rate at which the mass allocation between the two CDFs changes. If there are more than one point p such that $CC(p) = 0$, the above interpretations apply to each resulting region in $(0, 1)$. For details about properties and interpretations of PP and QQ plots, see Holmgren (1995) and Thas (2010).

Replacing in (2.2) the unknown $F(\cdot)$ by $\hat{F}_n(x) = n^{-1} \sum_{i=1}^n I(X_i \leq x)$, where $I(\omega)$ is the indicator function of event ω , leads to the *empirical CC*

$$(2.3) \quad \widehat{CC}(p) = \frac{p - \hat{F}_n(F_0^{-1}(p))}{\sqrt{p(1-p)}}, \quad p \in (0, 1).$$

Formally, $\widehat{CC}(p)$ is a consistent estimator of $CC(p)$ in the sense that, for any $\epsilon \in (0, 1)$, $\sup_{\epsilon \leq p \leq 1-\epsilon} |\widehat{CC}(p) - CC(p)| \rightarrow 0$ in probability. More importantly, $\sqrt{n} \widehat{CC}(p)$ is asymptotically $N(0, 1)$ under \mathbb{H}_0 for each p . Thus, in contrast with empirical PP and QQ plots, $\sqrt{n} \widehat{CC}(\cdot)$ captures discrepancies between the postulated model and the data with equal precision over the whole range of p . Evaluating $\sqrt{n} \widehat{CC}(\cdot)$ at points on a grid in $(0, 1)$ and representing these as bars over the grid points yields a *bar plot* (B plot), as introduced by Ledwina and Wyłupek (2012a,b) in a related problem. Obviously, $\sqrt{n} \widehat{CC}(\cdot)$ are noisy but the bars being correlated, their visual inspection will typically allow to approximately identify regions where the null model puts more probability mass, via a clustering of its quantiles, than the data seems to suggest, and reversely.

As an example of the usefulness of the $CC(\cdot)$, consider the smiling baby data set (Bhattacharjee & Mukhopadhyay, 2013). The data ($n = 55$) are the smiling times (in seconds) of an eight-week-old baby. According to various authors, the data could realistically be uniformly distributed over the interval $[0, \theta]$. Here, we take $\theta = 23.5$, a value close to the estimators investigated by Bhattacharjee & Mukhopadhyay (2013) and transform the data onto $[0, 1]$. Panel 1) of Figure 2.1 shows the empirical PP plot against the reference $U[0, 1]$ distribution (the 45-degree line) while Panel 2) represents the B plot of $\sqrt{n} \widehat{CC}(p)$ for $p \in \{1/32, \dots, 31/32\}$. Inspection of these bars shows a coincidence of the null and empirical quantiles in the neighbourhood of $p = 0.45$ ($\simeq 10.6$ in the original units), slightly to the left of the median under \mathbb{H}_0 . The shape of the sets of positive bars to the left and negative bars to the right of $p \simeq 0.45$ suggests that the central quantiles of the true distribution could be more clustered about this point than those of the null uniform. Thus the true distribution is perhaps less dispersed than the uniform and slightly shifted toward 0. Note that similar insight can be derived from the empirical PP plot (Panel 1) and QQ plot (not shown) of this data set. However, by making use of the null expectation and approximate homoscedasticity of $\widehat{CC}(\cdot)$ under \mathbb{H}_0 , the B plot allows an enhanced appraisal of these main features of the data. In particular, this B plot allows seeing for which quantiles of the null CDF $F_0(\cdot)$, the discrepancy with the data is unexpectedly large (positive or negative). The approach is developed in Section 3.4 for the null and composite case and discussed for the present case in Appendix A.6, where we revisit this data set.

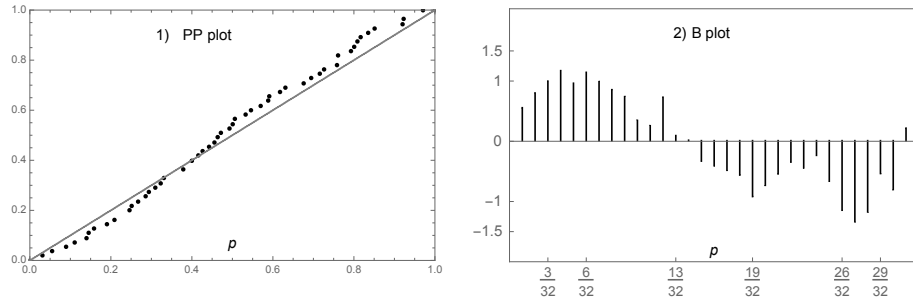


FIGURE 2.1. Graphical representations for the smiling baby data ($n = 55$) in Bhattacharjee & Mukhopadhyay (2013). Panel 1) : PP plot against the $U[0, 1]$ distribution (45-degree solid line) ; Panel 2): B plot of the $\sqrt{n} \widehat{CC}(\cdot)$ of eq. (2.3) evaluated over the grid $p \in \{1/32, \dots, 31/32\}$.

Such visual insights about the discordance of data with a null model is interesting, but must be completed by a GoF test for error control. Here we exploit the asymptotic behaviour of $\sqrt{n} \widehat{CC}(\cdot)$ under \mathbb{H}_0 to obtain inferential statements about the overall validity of the model. Hence, we now consider the problem of creating a GoF test based on the empirical CC . The expression for $\widehat{CC}(\cdot)$ may suggest considering an empirical process over $[0, 1]$, to which would be applied some variant of classical GoF test statistics (see Ćmiel et al. (2020) and references therein). However the use of such functionals of an empirical process blurs the links between the test statistic and its components. Hence, in this work we proceed in a simpler and more traditional way by considering $\widehat{CC}(p)$ evaluated at points p in a finite set. These points are associated with a partition of the interval $[0, 1]$, which we allow to become more and more dense as the sample size increases. They are described in the next subsection. Then, from the values of $\widehat{CC}(\cdot)$ evaluated at these points, we build a χ^2 -type test statistic. Finally, we introduce a selection rule to decide about the most useful subset of points, which is a highly non-trivial problem in the case of statistics of the present type.

2.2. Nested partition of $(0,1)$ and projected Haar functions $\{h_{s,j}(\cdot)\}$. Let $a_{s,k} = (2k - 1)/2^{s+1}$, $s = 0, 1, \dots$, $k = 1, 2, \dots, 2^s$. Associated with a sequence of sample sizes n , let $S(n)$ be a user-defined increasing sequence of integers. With s ranging in $\{0, 1, \dots, S(n)\}$ and $k \in \{1, 2, \dots, 2^s\}$, introduce in turn the sequence of nested sets of points in $(0, 1)$ corresponding to those $a_{s,k}$'s with $\{s = 0\}$, $\{s = 0, 1\}$, $\{s = 0, 1, 2\}, \dots$, sorted from smallest to largest to create the increasingly finer sets of points

$$\{p_{0,1}\}, \{p_{1,1}, p_{1,2}, p_{1,3}\}, \dots, \{p_{s,1}, \dots, p_{s,d(s)}\}, \dots \text{ where } d(s) = 2^{s+1} - 1.$$

For example, if $S(n) = 2$ the nested sets of ordered points are $\{4/8\}$, $\{2/8, 4/8, 6/8\}$ and $\{1/8, 2/8, 3/8, 4/8, 5/8, 6/8, 7/8\}$. Also define

$$\mathbb{D}(n) = \{d(s) : s = 0, \dots, S(n)\} \text{ and } D(n) = d(S(n)).$$

Now for a given s and corresponding $d(s)$, introduce the $d(s)$ -dimensional vector of functions $(h_{s,1}(p), \dots, h_{s,d(s)}(p))$ with $0 \leq p \leq 1$, where for $j \in \{1, \dots, d(s)\}$

$$\begin{aligned} h_{s,j}(p) &= -\sqrt{\frac{1 - p_{s,j}}{p_{s,j}}} I(0 \leq p \leq p_{s,j}) + \sqrt{\frac{p_{s,j}}{1 - p_{s,j}}} I(p_{s,j} < p \leq 1) \\ &= \frac{p_{s,j} - I(0 \leq p \leq p_{s,j})}{\sqrt{p_{s,j}(1 - p_{s,j})}}. \end{aligned}$$

These functions arise as normalized orthogonal projections of the Haar functions onto the cone of nondecreasing functions (cf. Ledwina & Wyłupek, 2012b) and constitute the building blocks of our tools. Obviously, the functions in this system are normalized but not orthogonal. The explicit form of the inner product matrix of the $h_{s,j}(\cdot)$ and its inverse have been derived in Ledwina & Wyłupek (2012b) under \mathbb{H}_0 . Note that Pearson's χ^2 is also related to a set of points $0 = \pi_0 < \pi_1 < \dots < \pi_k = 1$ defining the normalized but not orthogonal system of functions given by $l_j(p) = \{I(\pi_{j-1} < p < \pi_j) - (\pi_j - \pi_{j-1})\}/\sqrt{\pi_j - \pi_{j-1}}$. Here, a single $l_j(\cdot)$ corresponds to two neighbouring points, so Pearson's system is naturally adapted to histograms. This is to be contrasted with the system $\{h_{s,j}(\cdot)\}$, where each point $p_{s,j}$ corresponds to the single function $h_{s,j}(\cdot)$ and is thus adapted to CDFs.

2.3. Fourier coefficients of the comparison density in the system $\{h_{s,j}(\cdot)\}$. Write $f_0(\cdot)$ and $f(\cdot)$ for the densities of $F_0(\cdot)$ and $F(\cdot)$ respectively. Assume further that $f_0(x) = 0 \implies f(x) = 0$. Then the function $H(\cdot)$ satisfies $H(0) = 0$, $H(1) = 1$

and possesses a density, called the *comparison density* (Parzen, 2004) or the *relative density* (Handcock & Morris, 1999) given by

$$(2.4) \quad \kappa(p) = \frac{f(F_0^{-1}(p))}{f_0(F_0^{-1}(p))}, \quad p \in (0, 1).$$

Obviously, $\kappa(\cdot) \equiv 1$ if and only if \mathbb{H}_0 holds. Now, consider the Fourier coefficients (FC) of $\kappa(\cdot)$ in the system $\{h_{s,j}(\cdot)\}$. The (s, j) -th Fourier coefficient, noted $\gamma_{s,j}$, takes the form

$$(2.5) \quad \gamma_{s,j} = \gamma_{s,j}(p_{s,j}) = \int_0^1 \kappa(p) h_{s,j}(p) dp.$$

Then, \mathbb{H}_0 can be equivalently reformulated as $\gamma_{s,j} = 0$, $s = 0, 1, \dots, j = 1, \dots, d(s)$.

Expression (2.5) leads to the empirical FC : $\hat{\gamma}_{s,j} = n^{-1} \sum_{i=1}^n h_{s,j}(F_0(X_i))$. A little algebra shows that $\gamma_{s,j} = CC(p_{s,j})$ and $\hat{\gamma}_{s,j} = \widehat{CC}(p_{s,j})$. These relationships shed further light on how $CC(p)$ and its empirical version operate. The form of the $h_{s,j}(\cdot)$'s shows that $CC(\cdot)$ essentially contrasts the reweighted probability mass, induced by $\kappa(\cdot)$, of the interval $(0, p]$ to that of $(p, 1]$ as compared to the $U(0, 1)$. Observe that, in view of our nested partition, increasing s allows for more and more careful checks of the discrepancies between $F(\cdot)$ and $F_0(\cdot)$. More precisely, we start by considering the deviation at the median of $F_0(\cdot)$, then check the fit at its quartiles and so on. Also, $\hat{\gamma}_{s,j}$ can be seen as a statistic for testing $\gamma_{s,j} = 0$.

For $S(n)$ large enough corresponding to $n \geq n_0$ say, note that if $F(\cdot) \neq F_0(\cdot)$, there exist $s_0 \in \{0, 1, \dots, S(n)\}$ and $j_0 \in \{1, \dots, d(s_0)\}$ such that

$$(2.6) \quad \gamma_{s_0, j_0} = \frac{p_{s_0, j_0} - F(F_0^{-1}(p_{s_0, j_0}))}{\sqrt{p_{s_0, j_0}(1 - p_{s_0, j_0})}} \neq 0.$$

Because we are considering nested partitions, for $n \geq n_0$ and $s \geq s_0$, there is a corresponding j_0 such that (2.6) remains valid; hence we might as well assume that n_0, s_0, j_0 are the smallest values for which (2.6) holds.

2.4. χ^2 -type test statistic and selection rule for its number of components $d(s)$. Set

$$(2.7) \quad \mathcal{K}(d(s)) = \sqrt{n} (\widehat{CC}(p_{s,1}), \dots, \widehat{CC}(p_{s,d(s)})).$$

This vector can be seen as the score vector of an auxiliary parametric model associated with $(h_{1,1}(p), \dots, h_{s,d(s)}(p))$ modelling an alternative to $F_0(\cdot)$. Consider the χ^2 -type test statistic for the GoF problem of testing \mathbb{H}_0 :

$$(2.8) \quad \mathcal{P}_{d(s)} = \mathcal{K}(d(s)) \mathcal{K}'(d(s)) = n \sum_{j=1}^{d(s)} \left[\widehat{CC}(p_{s,j}) \right]^2.$$

Under \mathbb{H}_0 , the null asymptotic distribution of $\mathcal{P}_{d(s)}$ is a sum of weighted χ_1^2 . The covariance matrix of $\mathcal{K}(d(s))$ and its related score statistic could be used to obtain a quadratic form with an asymptotic $\chi_{d(s)}^2$ distribution. We do not pursue this further because this matrix being non-diagonal, the components of the quadratic form are linear combinations of the $\widehat{CC}(p_{s,j})$ and thus difficult to interpret. Furthermore, the convenience of a $\chi_{d(s)}^2$ reference distribution vanishes in view of the upcoming enhancements to (2.8).

An important question with GoF test statistic (2.8) is the proper choice for the number of components $d(s)$ to include. Here we adapt a data driven selection rule inspired by Ledwina & Wyłupek (2012a, 2015) that is defined as follows. First, consider the selection rule with AIC-type penalty

$$(2.9) \quad A(a) = \min \{d(s) \in \mathbb{D}(n) : \mathcal{P}_{d(s)} - a \cdot d(s) \geq \mathcal{P}_{d(t)} - a \cdot d(t), d(t) \in \mathbb{D}(n)\}.$$

Now, given n and significance level α , find by the Monte Carlo method a value $a = a(n, \alpha)$ such that, under \mathbb{H}_0 , $\text{pr}(A(a) = 1) \geq 1 - \alpha$. Note that such a value exists because $\text{pr}(A(a) = 1)$ is a nondecreasing function of $a \in [0, \infty)$. Then introduce the auxiliary statistic

$$(2.10) \quad \mathcal{M}_{D(n)} = \max_{1 \leq j \leq D(n)} \left| \sqrt{n} \widehat{CC}(p_{S(n),j}) \right|$$

and denote by $m(n, \alpha)$ the critical value of the α -level test rejecting \mathbb{H}_0 for large values of $\mathcal{M}_{D(n)}$. Finally, set

$$(2.11) \quad R(\alpha) = \begin{cases} A(a(n, \alpha)) & \text{if } \mathcal{M}_{D(n)} \leq m(n, \alpha), \\ A(0) & \text{otherwise.} \end{cases}$$

With these notations, our data driven GoF χ^2 -type test statistic takes the form $\mathcal{P}_{R(\alpha)}$. Its critical values are obtained via Monte Carlo simulations (see Appendix B for some recommendations).

In (2.11), test statistic $\mathcal{M}_{D(n)}$ acts like an oracle. When the oracle, after globally examining the large number of components in $\mathcal{M}_{D(n)}$, sees no reason to reject \mathbb{H}_0 , the procedure proceeds to look at a smaller subset of components with the idea that a more directional analysis may provide reasons to reject. When the oracle rejects, the procedure basically seeks confirmation by using the comprehensive test statistic $\mathcal{P}_{D(n)}$. Note that under \mathbb{H}_0 the oracle will seldom reject. This generates moderately large critical values, which in turn leads to more frequent rejections under the alternative and thus high power.

It remains to show that a test based on $\mathcal{P}_{R(\alpha)}$ is consistent. The following proposition is proved in Appendix D.1.

Proposition 1. *Assume that $S(n) \rightarrow \infty$ and $D(n) = o(n^{2\delta})$ for some $\delta \in (0, 1/2)$. Then the test rejecting for large values of $\mathcal{P}_{R(\alpha)}$ is consistent under any alternative $F(\cdot) \neq F_0(\cdot)$.*

2.5. A simulation experiment. In order to assess the properties of our test based on $\mathcal{P}_{R(\alpha)}$, a simulation experiment was performed. The goal was to compare the power of $\mathcal{P}_{R(\alpha)}$ with some of its competitors. The null hypothesis considered is $F_0(x) = \Phi(x)$, the CDF of the $N(0, 1)$ distribution. The alternatives were carefully selected to cover a fair range of shapes of $CC(\cdot)$, see Figure 2.2 and the discussion in Appendix C. They are:

- $\mathbb{A}_1^0(\theta)$, a normal location model with CDF $\Phi(x - \theta)$, $\theta \in \mathbb{R}$;
- $\mathbb{A}_2^0(\theta)$, a normal scale model with CDF $\Phi(x/(1 + \theta))$, $\theta > -1$;
- $\mathbb{A}_3^0(\theta)$, the two-piece normal distribution with density $C\{I(x < 0)\exp(-x^2/2) + I(x \geq 0)\exp(-x^2/2(1 + \theta)^2)\}$ with $C = (\sqrt{2\pi}(2 + \theta)/2)^{-1}$ and $\theta > -1$;
- $\mathbb{A}_4^0(\theta)$, a model of Fan with local departure around 0 and density $\phi(x)[1 + \{4z\theta^{-2}(\theta - |z|)\}I(|z| < \theta)]$, where $z = 2\Phi(x) - 1$ and $\theta \in [0, 1]$;
- $\mathbb{A}_5^0(\theta)$, a normal contamination model with CDF $(1 - \theta)\Phi(x) + \theta\Phi(x - 2)$, $\theta \in [0, 1]$;
- $\mathbb{A}_6^0(\theta)$, Anderson's skewed distribution with stochastic representation $I(Z < 0)Z/(1 - \theta) + I(Z \geq 0)Z(1 - \theta)$ where $Z \sim N(0, 1)$ and $\theta \in [0, 1]$;
- $\mathbb{A}_7^0(\theta)$, the Mason & Schuenemeyer tail alternative with CDF $H(\Phi(x), q, \theta)$ where $\theta > -1$, $H(x, q, \theta) = (q^{\theta/(\theta+1)}x^{1/(\theta+1)})I(0 \leq x < q) + xI(q \leq x \leq 1 - q) + ((1 - q^{\theta/(\theta+1)})(1 - x)^{1/(\theta+1)})I(1 - q < x \leq 1)$ and here $q = 0.25$;
- $\mathbb{A}_8^0(\theta)$, Anderson's kurtotic distribution generated as $X = Z \times |Z|^\theta$, where $Z \sim N(0, 1)$ and $\theta \geq 0$;

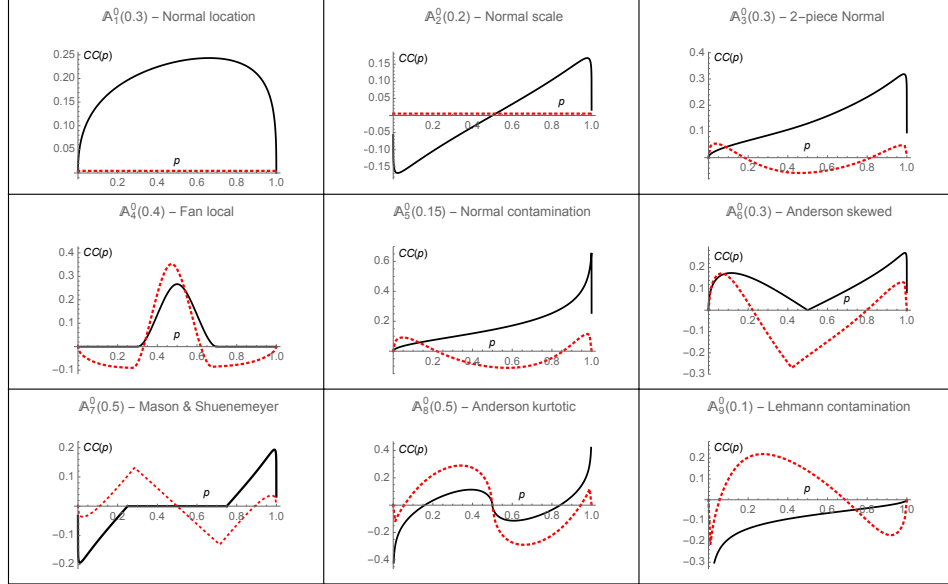


FIGURE 2.2. $CC(p)$, $p \in (10^{-5}, 1-10^{-5})$ (solid black curve) for the alternative distributions in Table 1 for testing the simple null hypothesis $\mathbb{H}_0 : \Phi(x)$. The red dotted curve represents $CC(\cdot; \beta(F))$ of (3.3) corresponding to the null model $\Phi((x - \beta_1)/\beta_2)$ with (β_1, β_2) unknown.

- $A_9^0(\theta)$, a Lehmann contamination model with CDF $(1-\theta)\Phi(x) + \theta(\Phi(x))^{0.175}$, $\theta \in [0, 1]$ with $(\Phi(x))^\delta$ being the Lehmann distribution.

For more details about these alternatives, see Appendix C. They all reduce to the $N(0, 1)$ when $\theta = 0$ and thus embed the null model. Note that our choice for \mathbb{H}_0 offers the convenience of easily defined embedding families of alternatives and allows some comparisons with the simulations in Appendix C. No loss of generality ensues from this choice as the probability integral transformation translates the GoF problem for any continuous $F_0(\cdot)$ into a null $U(0, 1)$ distribution, for which many good tests have been derived. In particular, we have considered the following two competitors: the Anderson-Darling statistic (AD) and the Berk-Jones (1979) statistic (BJ).

Taking $\alpha = 0.05$ and $n = 100$, we investigated $\mathcal{P}_{R(\alpha)}$ with $S(n) = 6$ and computed $m(n, \alpha) = 3.30$ and $a(n, \alpha) = 3.31$ (see Appendix B for some practical considerations regarding these choices and values). The power functions for the nine alternatives were simulated in their θ range for each of AD, BJ and $\mathcal{P}_{R(\alpha)}$. The 5% critical values were obtained from 100 000 replications under the null distribution, while the powers were computed from 10 000 Monte Carlo runs. We extracted from each power curve a representative value of θ which provided intermediate powers, e.g. not too close to 0.05 and 1.0 and where the powers of the various tests could be distinguished. As a result of these choices, the powers presented below offer a comprehensive view of the comparative behaviour of the tests over a fair range of situations.

The results are reported in Table 1. None of the tests always dominate and $\mathcal{P}_{R(\alpha)}$ emerges as very competitive. In most cases, AD is less powerful and simulations

Alternative	AD	BJ	\mathcal{M}_{127}	$\mathcal{P}_{R(\alpha)}$
$\mathbb{A}_1^0(0.3)$	83	69	65	77
$\mathbb{A}_2^0(0.2)$	35	51	59	58
$\mathbb{A}_3^0(0.3)$	67	73	78	79
$\mathbb{A}_4^0(0.4)$	27	47	39	39
$\mathbb{A}_5^0(0.15)$	83	92	93	94
$\mathbb{A}_6^0(0.3)$	49	65	63	64
$\mathbb{A}_7^0(0.5)$	24	54	63	59
$\mathbb{A}_8^0(0.5)$	47	88	80	80
$\mathbb{A}_9^0(0.1)$	53	90	79	75

TABLE 1. Powers ($n = 100$, $\alpha = 0.05$) of the Anderson-Darling (AD), the Berk-Jones (BJ), the oracle $\mathcal{M}_{D(n)}$ with $D(n) = 127$ and our $\mathcal{P}_{R(\alpha)}$ tests for $\mathbb{H}_0 : F(x) = \Phi(x)$ against a set of balanced alternatives.

results in Ćmiel et al. (2020) show that for larger sample sizes, the power differences between AD and $\mathcal{M}_{D(n)}$ can be even more pronounced. Thus powerwise, we conclude that our test could be included among the best solutions for this problem.

We close this section by noting that when any of AD, BJ rejects \mathbb{H}_0 , the user is left with little clues as to what aspects of the null model must be corrected. In contrast, when the competitive $\mathcal{P}_{R(\alpha)}$ rejects, a B plot as in Panel 2) of Figure 2.1 can be produced to help the user see where the, now established, discrepancies are located. The B plot could be further supplemented with acceptance regions to separate in a reasonable way the large components from those more consonant with a local agreement to the model. This will be discussed in Section 3.3 and illustrated in Section 3.5 (see also Appendix A). Hence the pair (B plot, $\mathcal{P}_{R(\alpha)}$) can be a useful tool for statistical modelling. We now consider the more common case where the parameter β in model $F_0(\cdot; \beta)$ is unknown.

3. COMPOSITE NULL HYPOTHESIS

3.1. Fourier coefficients and empirical CC. In the case of a composite null hypothesis, we proceed in a reversed order than under \mathbb{H}_0 . We start with a counterpart to the empirical Fourier coefficients (FC) associated with an adjusted variant of $\hat{\gamma}_{s,j}$ to motivate our definition of an analogue to $CC(\cdot)$ in the present setting. Next, we define the related χ^2 -type test and its data driven version. We focus on the important case of location-scale families and illustrate our approach by testing GoF to the Gaussian distribution. A simulation experiment confirms that our test is competitive in a broad spectrum of situations. Finally, we produce the B plot of a real data set (more are worked out in Appendix A) to show their usefulness in obtaining insights about the aspects of the model that could have caused rejection.

Let X_1, \dots, X_n be i.i.d. observations from a continuous CDF $F(\cdot)$ and consider the family of null models $F_0(\cdot; \beta)$ where the parameter $\beta \in \mathcal{B}$ is unknown. The null hypothesis of interest is composite and takes the form

$$(3.1) \quad \mathbb{H} : F(\cdot) = F_0(\cdot; \beta) \text{ for some } \beta \in \mathcal{B}.$$

As in Section 2.3, the (s, j) -th empirical FC of the comparison density associated with $F(\cdot)$ and $F_0(\cdot; \beta)$ can be defined as

$$\hat{\gamma}_{s,j}(\beta) = \hat{\gamma}_{s,j}(p_{s,j}; \beta) = \frac{1}{n} \sum_{i=1}^n h_{s,j}(F_0(X_i; \beta)).$$

Plugging into this expression the value $\tilde{\beta}$ of an estimator of β , elementary calculations yield

$$(3.2) \quad \hat{\gamma}_{s,j}(\tilde{\beta}) = \frac{p_{s,j} - \bar{F}_n(p_{s,j}; \tilde{\beta})}{\sqrt{p_{s,j}(1 - p_{s,j})}}, \quad \text{where} \quad \bar{F}_n(p; \tilde{\beta}) = n^{-1} \sum_{i=1}^n I(F_0(X_i; \tilde{\beta}) \leq p).$$

From there, it is tempting to define the empirical CC as in (3.2). However, the use of $\tilde{\beta}$ must be taken into account. Consider the empirical process $\bar{e}_n(p; \tilde{\beta}) = \sqrt{n}(\bar{F}_n(p; \tilde{\beta}) - p)$, $p \in [0, 1]$. Durbin (1973) has studied this process and shown that under mild assumptions on $\tilde{\beta}$ and $F_0(\cdot; \cdot)$, it converges under \mathbb{H} to some Gaussian process on $[0, 1]$ with 0 mean function. The covariance function $\rho(\cdot, \cdot)$ of the limiting process is also given in Durbin (1973). Hence, putting $\sigma_{s,j} = \sqrt{\rho(p_{s,j}, p_{s,j})}$, we get that $\bar{e}_n(p_{s,j}; \tilde{\beta})/\sigma_{s,j}$ is asymptotically $N(0, 1)$ under \mathbb{H} . This leads to defining the empirical CC in the present context as

$$\widehat{CC}(p; \tilde{\beta}) = \frac{p - \bar{F}_n(p; \tilde{\beta})}{\sqrt{\rho(p, p)}}.$$

3.2. CC and alternatives in the case of location-scale models. Let $F(\cdot)$ be the true CDF of the data and suppose the null model is location-scale with β estimated by $\tilde{\beta}$, a \sqrt{n} -consistent estimator under $F_0(\cdot; \cdot)$. Suppose that under $F(\cdot)$, $\tilde{\beta} \rightarrow \beta(F) = (\beta_1(F), \beta_2(F))$ where the convergence is in probability with respect to $F(\cdot)$. When β_1 and β_2^2 are estimated by MLE, these are the expectation and standard deviation of $F(\cdot)$ provided its fourth moment is finite. The population version of $\widehat{CC}(p; \tilde{\beta})$ is given by

$$(3.3) \quad CC(p; \beta(F)) = \frac{p - F\left(\beta_2(F) \times F_0^{-1}(p) + \beta_1(F)\right)}{\sqrt{\rho(p, p)}}.$$

We call $F(\cdot)$ an alternative when $F(x) \neq F_0((x - \beta_1(F))/\beta_2(F))$ for some $x \in \mathbb{R}$. By continuity of $F(\cdot)$ and the fact that the partition of Section 2.2 is dense, there exist $n_0, s_0 \in \{0, \dots, S(n_0)\}$ and $j_0 \in \{1, \dots, d(s_0)\}$, such that $CC(p_{s_0, j_0}; \beta(F)) \neq 0$. Without loss of generality we may, as in Section 2.3, assume that n_0, s_0, j_0 are the smallest such indices. Thus for sufficiently large n , there will be at least one non-zero component among the $CC(p_{s,j}; \beta(F))$. Hence, test statistic (3.6) below is expected to be consistent under a large spectrum of alternatives.

Consider the important sub-case where $F_0(x; \beta) = F_0((x - \beta_1)/\beta_2)$ is the Gaussian CDF with unknown expectation β_1 and variance β_2^2 , i.e. $F_0(\cdot) = \Phi(\cdot)$ with density $f_0(\cdot) = \varphi(\cdot)$. When β_1 and β_2^2 are estimated by MLE, i.e. $\tilde{\beta}_1 = \bar{X}$ and $\tilde{\beta}_2^2 = S^2 = n^{-1} \sum_{i=1}^n (X_i - \bar{X})^2$, we have $\rho(t, v) = \min\{t, v\} - tv - \rho_1(t)\rho_1(v) - \rho_2(t)\rho_2(v)$, $t, v \in [0, 1]$, where $\rho_1(t) = \varphi(\Phi^{-1}(t))$ and $\rho_2(t) = 1/\sqrt{2} \varphi(\Phi^{-1}(t))\Phi^{-1}(t)$. In this case, the quantity $\sigma_{s,j} = (p_{s,j}(1 - p_{s,j}) - \rho_1^2(p_{s,j}) - \rho_2^2(p_{s,j}))^{1/2}$ is smaller than the value $\sqrt{p_{s,j}(1 - p_{s,j})}$ adequate for \mathbb{H}_0 . To be specific, $\rho(t, t)$ is much smaller than $t(1 - t)$ in $(0, 1)$, while $\lim_{t \rightarrow 0+} \rho(t, t)/[t(1 - t)] = \lim_{t \rightarrow 1-} \rho(t, t)/[t(1 - t)] = 1$.

3.3. The bar plot (B plot) in the composite and simple null cases. We start by stating the following simple fact about B plots in the composite case, whose proof is in Appendix D.3.

Remark 1. *Under the assumptions on $F(\cdot)$ and $\tilde{\beta}$ in Proposition 2 below, it holds that, as $n \rightarrow \infty$, $\sup_{\epsilon \leq p \leq 1-\epsilon} |\widehat{CC}(p; \tilde{\beta}) - CC(p; \beta(F))| \rightarrow 0$ in probability for any $\epsilon \in (0, 1)$.*

Next and similarly to the case of Section 2.1 where $\beta(F)$ is known, note that $CC(p; \beta(F))$ inherits its interpretation from its local sign and possible zeroes. Now

$F_0(\cdot, \beta(F))$ is the reference CDF. Therefore, it is important to discriminate those bars that seem compatible with \mathbb{H} from more surprisingly large ones, positive or negative. This suggests supplementing the B plot with one-sided α -th acceptance intervals for the height of individual bars expected under the null model. Here, this is done by drawing on the B plot horizontal lines at ± 1.645 , if one considers $\alpha = 0.05$. We use asymptotic critical levels because they approximate well the finite sample distribution of single bars; see Appendix A.1 for some related comments.

For subsets of bars, recall from Durbin's (1973) result that the joint asymptotic distribution of a set of components is multivariate normal with means 0, unit variances and associated covariance function. Thus the correlation between the bars must be taken into account. When a set of bars, say $\sqrt{n} \widehat{CC}(p_{S(n),j}; \tilde{\beta})$ for $j \in \{r, \dots, s\}$, are jointly positive, one approach to flag their significance is to compute a one-sided simultaneous α -level acceptance region. This consists in computing by Monte Carlo and under \mathbb{H} an approximation to $u(n, \alpha; \{r, \dots, s\})$ in

$$(3.4) \quad \text{pr}\left(\max_{r \leq j \leq s} \sqrt{n} \widehat{CC}(p_{S(n),j}; \tilde{\beta}) \leq u(n, \alpha; \{r, \dots, s\})\right) \geq 1 - \alpha.$$

Of course, if the bars under consideration are negative, (3.4) must be adapted to obtain the lower bound $\ell(n, \alpha; \{r, \dots, s\})$ via

$$\text{pr}\left(\min_{r \leq j \leq s} \sqrt{n} \widehat{CC}(p_{S(n),j}; \tilde{\beta}) \geq \ell(n, \alpha; \{r, \dots, s\})\right) \geq 1 - \alpha.$$

Such computations are easily done because with a location-scale null model, the distribution of $\widehat{CC}(p_{S(n),j}; \tilde{\beta})$ does not depend on β , so sampling can be made from e.g. a $N(0, 1)$. When β is known, a variant of $u(n, \alpha; \{r, \dots, s\})$ can be computed by approximating under the null hypothesis expression (3.4) using $\widehat{CC}(p_{S(n),j})$, and similarly for $\ell(n, \alpha; \{r, \dots, s\})$. When at least one of the bars related to $\{r, \dots, s\}$ is above the computed $u(n, \alpha; \{r, \dots, s\})$ or below $\ell(n, \alpha; \{r, \dots, s\})$, this indicates that the data seems incompatible with the null model in the related region. We represent these simultaneous acceptance regions by shaded gray stripes on the B plot, see Section 3.5 and Appendix A for illustrations. Note that r, s should be non-random to allow statements controlling Type I errors.

3.4. χ^2 -type test statistic and a selection rule for $d(s)$ for testing Gaussianity.

Consider as in (2.7),

$$\mathcal{K}(\tilde{\beta}, d(s)) = \sqrt{n} \left(\widehat{CC}(p_{s,1}; \tilde{\beta}), \dots, \widehat{CC}(p_{s,d(s)}; \tilde{\beta}) \right).$$

Inspired by (2.8), a GoF test statistic for \mathbb{H} is

$$(3.5) \quad \mathcal{P}_{d(s)}(\tilde{\beta}) = \mathcal{K}(\tilde{\beta}, d(s)) \mathcal{K}'(\tilde{\beta}, d(s)) = n \sum_{j=1}^{d(s)} \left[\widehat{CC}(p_{s,j}; \tilde{\beta}) \right]^2.$$

Remark 2. When $F_0(\cdot; \beta)$ is a location-scale family, i.e. $F_0(x; \beta) = F_0((x - \beta_1)/\beta_2)$ with $\beta = (\beta_1, \beta_2) \in \mathcal{B} \subseteq \mathbb{R} \times \mathbb{R}_+$, we have $\bar{F}_n(p; \tilde{\beta}) = \hat{F}_n(\tilde{\beta}_2 F_0^{-1}(p) + \tilde{\beta}_1)$, where $\hat{F}_n(\cdot)$ is the ordinary empirical CDF of the sample. The process $\bar{e}_n(p; \tilde{\beta})$ then has a limiting distribution that does not depend on β . Test statistic (3.5) becomes

$$(3.6) \quad \mathcal{P}_{d(s)}(\tilde{\beta}) = n \sum_{j=1}^{d(s)} \left[\frac{p_{s,j} - \hat{F}_n(\tilde{\beta}_2 F_0^{-1}(p_{s,j}) + \tilde{\beta}_1)}{\sigma_{s,j}} \right]^2.$$

To reduce technicalities, we assume in the present section that $\mathbb{H} : F(x) = \Phi((x - \beta_1)/\beta_2)$, i.e. we consider testing GoF to the Gaussian distribution. Estimate β by the MLE $\tilde{\beta} = (\bar{X}, S^2)$. To define a selection rule for $d(s)$ in (3.6), we proceed similarly as in Section 2.4. First, we seek an oracle test whose task is to provide

some reliable preliminary information on the situation. The results of Section 2 suggest considering the following version of the oracle test (2.10), namely

$$(3.7) \quad \mathcal{M}_{D(n)}(\tilde{\beta}) = \max_{1 \leq j \leq D(n)} \left| \sqrt{n} \widehat{CC}(p_{S(n),j}; \tilde{\beta}) \right|.$$

However, it turns out (see Table C.2 in Appendix C), that this test is powerwise inferior to some recommended test procedures in the composite context. The use of selection rules based on this oracle leads to data driven tests which are noticeably more powerful than $\mathcal{M}_{D(n)}(\tilde{\beta})$, but still not competitive with the best existing solutions. This is a manifestation of the difficulties encountered in moving from a simple to a composite null hypothesis in the present problem.

Instead, we base our selection rule on the oracle test

$$\mathcal{R}_n = 1 - \frac{\hat{\sigma}_n^2}{S^2}, \quad \text{where } \hat{\sigma}_n = \int_0^1 \hat{F}_n^{-1}(t) \Phi^{-1}(t) dt,$$

where large observed values of $\mathcal{T}_n = n \mathcal{R}_n$ are significant. This test statistic, which we refer to as BCMR, has been introduced in del Barrio et al. (1999) and further studied in Csörgő (2003), among others. The surrounding theory regarding this test allows its adaptation to some other composite null hypotheses. Hence, the solution below can serve as a template in a variety of important cases.

Introduce

$$A(a; \tilde{\beta}) = \min \left\{ d(s) \in \mathbb{D}(n) : \mathcal{P}_{d(s)}(\tilde{\beta}) - a \cdot d(s) \geq \mathcal{P}_{d(t)}(\tilde{\beta}) - a \cdot d(t), d(t) \in \mathbb{D}(n) \right\}.$$

Now, given n and α , find by the Monte Carlo method a value $a = a(n, \alpha; \tilde{\beta})$ such that, under \mathbb{H} , $\text{pr}(A(a(n, \alpha; \tilde{\beta})) = 1) \geq 1 - \alpha$. Finally, let $t(n, \alpha)$ be the α -level critical value of \mathcal{T}_n and set

$$\tilde{Q}(\alpha) = \begin{cases} A(a(n, \alpha; \tilde{\beta}); \tilde{\beta}) & \text{if } \mathcal{T}_n \leq t(n, \alpha), \\ A(1.5; \tilde{\beta}) & \text{otherwise.} \end{cases}$$

Notice that the penalty in the case $\mathcal{T}_n > t(n, \alpha)$ differs from that in (2.11). The reason for this is explained in Appendix B. $\tilde{Q}(\alpha)$ can be seen as an adaptation of the selection rule A in Ledwina & Wyłupek (2015) introduced in the context of data driven test associated with transformed Hermite polynomials.

With these notations, the data driven GoF χ^2 -type test statistic for the null hypothesis \mathbb{H} takes the form $\mathcal{P}_{\tilde{Q}(\alpha)}(\tilde{\beta})$. Some of its critical values $\tilde{c}(n, \alpha)$ are listed in Appendix B and others can be obtained via linear interpolation or Monte Carlo simulations. The following proposition is proved in Appendix D.2.

Proposition 2. *Let $F(\cdot)$ be an alternative in the sense of Section 3.2 to the Gaussian null model. Assume that the fourth moment of $F(\cdot)$ exists and is finite. Moreover, assume that $F(\cdot)$ possesses a bounded density $f(\cdot)$ with respect to the Lebesgue measure on \mathbb{R} . Further assume that $\tilde{\beta}$ is the MLE for β . Finally, let $S(n) \rightarrow \infty$ and $D(n) = o(n^{1/2})$ as $n \rightarrow \infty$. Then, the test rejecting for large values of $\mathcal{P}_{\tilde{Q}(\alpha)}(\tilde{\beta})$ is consistent under $F(\cdot)$.*

In order to assess the properties of the test based on $\mathcal{P}_{\tilde{Q}(\alpha)}(\tilde{\beta})$, a simulation experiment was performed. The structure of the experiment mimics closely that in Section 2.5. The null hypothesis is $\mathbb{H} : F(x) = \Phi((x - \beta_1)/\beta_2)$ where (β_1, β_2^2) are estimated by MLE. For this problem, several solutions exist (see Arnastauskaité et al., 2021), notably the Anderson-Darling (AD), the Shapiro-Wilks (SW) and the BCMR tests.

Our main interest is to see how our approach compares with these. The details and results of the simulation appear in Appendix C, which pertains to a set of carefully selected alternatives according to the form of their $CC(p; \beta(F))$, partly inspired by those in Section 2.5. It emerges from this experiment that, as an oracle, $\mathcal{M}_{D(n)}(\tilde{\beta})$ generally does poorly. Otherwise, and similarly to the context of Section 2, none of the other tests dominates and $\mathcal{P}_{\tilde{Q}(\alpha)}(\tilde{\beta})$ turns out to be a good competitor, being powerwise on par with the oracle test it is based upon. Recall that a main advantage is the possibility of deriving information from the B plot about where the null model could be at fault and an overall measure of fit based on this plot.

3.5. A real data example: wave records. The results of the previous sections are now applied to a real data set to show how useful insights can be derived from the components $\sqrt{n} \widehat{CC}(\cdot; \tilde{\beta})$ when using the methods of the paper. More examples are worked out in Appendix A.

We consider a data set in Bickel and Doksum (1977, p. 384, Table 9.6.3) measuring the time spent above a high level of $n = 66$ wave records in the San Francisco bay. Their analysis does not reject the null Gaussian hypothesis at level 10%. The data were later considered by Rosenkranz (2000) whose simultaneous 90% confidence band approach indicates some inconsistency with the postulated Gaussian model in the left tail of the distribution. They were reexamined by Aldor-Noiman et al. (2013) using simultaneous confidence bands about the QQ plot. Their approach detects, at the 5% level, a significant departure from normality in the right tail, while another approach, based on Kolmogorov-Smirnov bands, nearly rejects, at the same level, relying solely on points at the centre of the data.

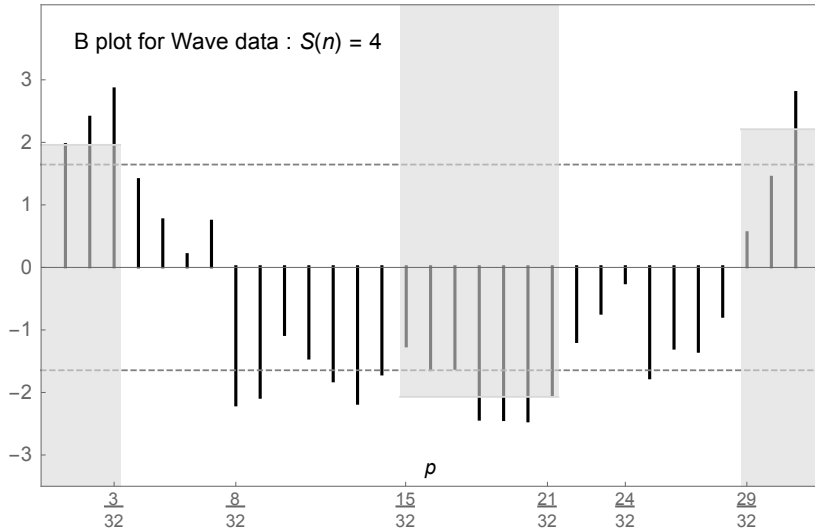


FIGURE 3.1. B plot of $\sqrt{n} \widehat{CC}(p_{4,j}; \tilde{\beta})$, with $j \in \{1, \dots, 31\}$, for the wave records data ($n = 66$) in Bickel & Doksum (1997). The dashed gray lines are located at ± 1.645 to identify the individual bars where some dissonance with \mathbb{H} : *Gaussianity* occurs at one-sided level 5%. The shaded gray stripes are the simultaneous 5% one-sided acceptance regions for subsets of bars $\{1, 2, 3\}$, $\{15, \dots, 21\}$ and $\{29, 30, 31\}$.

For this data set, we have $\tilde{\beta}_1 = \bar{X} = 3.79$ and $\tilde{\beta}_2 = S = 2.39$. We apply the test based on $\mathcal{P}_{\tilde{Q}(\alpha)}(\tilde{\beta})$ with $\alpha = 0.05$, $S(n) = 4$, $t(n, \alpha) = 2.60$ and compute $a(n, \alpha; \tilde{\beta}) = 3.18$. The observed value of \mathcal{T}_n is 4.52, leading to $\tilde{Q}(\alpha) = 31$ and $\mathcal{P}_{\tilde{Q}(\alpha)}(\tilde{\beta}) = 92.40$ to be compared to the 5% critical level of 10.46 obtained from 100 000 Monte Carlo replications. Thus we reject the null hypothesis of Gaussianity at the 5% level. The tests AD, SW and BCMR also reject at the 5% level with p -values of 0.004 for AD, 0.002 for SW and 0.002 for BCMR. Figure 3.1 shows the B plot of $\sqrt{n} \widehat{CC}(p_{4,j}; \tilde{\beta})$ with $j \in \{1, \dots, 31\}$ along with the ± 1.645 lines delimiting the one-sided upper and lower 0.05-level asymptotic individuals acceptance regions (dashed horizontal lines in Figure 3.1).

The values of $\sqrt{n} \widehat{CC}(p_{4,j}; \tilde{\beta})$ above and below the dashed lines support the finding of Aldor-Noiman et al. (2013) of a fatter right tail than a Gaussian distribution. Assuming that the meaning of their term “right tail” relates to quantiles such that $p \geq 29/32 \approx 0.9$, we can substantiate this by computing from (3.4) $u(66, 0.05; \{29, 30, 31\}) = 2.21$. From Figure 3.1, because the bar at $p = 31/32$ is above 2.21, this supports the claim of Aldor-Noiman et al. (2013). Note that such ranges for $p_{S(n),j}$ can be translated into the original data via $\tilde{\beta}_2 \Phi^{-1}(p_{S(n),j}) + \tilde{\beta}_1$, see Appendix A.1.

If we define similarly the left tail as below the first decile, i.e. $p \leq 3/32$, we get $u(66, 0.05; \{1, 2, 3\}) = 1.96$. Again from Figure 3.1, all three bars in $\{1, 2, 3\}$ are above this value, in agreement with the finding in Rosenkranz (2000) regarding a thinner than Gaussian left tail.

Finally, Aldor-Noiman et al. (2013) do not define the meaning of “centre of the data” but, in view of the above findings of a thinner left and fatter right tail, suggesting some asymmetry to the right, we have decided to consider a slightly shifted centre ranging from $0.45 \approx 15/32 \leq p \leq 21/32 \approx 0.65$. This yields $\ell(66, 0.05; \{15, \dots, 21\}) = -2.07$. The fact that three bars in this centre are below this value is consonant with the claim that, in this region, observations tend to be stochastically smaller than expected under Gaussianity. Appendix A.1 gives more details and some further analysis regarding this data set.

4. DISCUSSION

The present work proposes an approach for model validation based on the pair (B plot, $\mathcal{P}_{R(\alpha)}$) or (B plot, $\mathcal{P}_{\tilde{Q}(\alpha)}(\tilde{\beta})$) that appears to be a good compromise to the two routes presented in the introduction. In the case of a Gaussian null model, the test statistics are powerwise competitive with some of the best solutions proposed in the literature, while the B plot and related acceptance regions offer an enhanced assessment, with respect to PP or QQ plots, as to where the data deviate from the contemplated model. The technical details here are confined to the Gaussian null model. But existing evidence and earlier experience allows to expect that our approach can be extended to other location-scale families and several more complex models. In particular, other \sqrt{n} -consistent estimators than the MLE could be covered by adjusting the test statistic and the data driven selection procedure. For illustration of different situations where data driven smooth tests, using other systems of functions than the present $\{h_{s,j}(\cdot)\}$, work well see Kallenberg & Ledwina (1997), Peña (2003), Ducharme & Fontez (2004), Ducharme & Lafaye de Micheaux (2004, 2020), Inglot & Ledwina (2006), Bissantz et al. (2009), Escanciano & Lobato (2009), Janic & Ledwina (2009), Wang & Qu (2009) and Thas et al. (2015). It should be noted that in such situations, the constructions are more involved as a rule and additional technical work is needed.

In Sections 2.5 and 3.3, we have qualified our alternatives, chosen on a fair range of shape of CC 's, as “carefully” selected. See Appendix C for a discussion as to why this should be of some concern. More importantly, we discuss in some examples of Appendix A how the B plot can help in choosing an adequate GoF test strategy to formally assess the overall fit of data to a postulated model.

REFERENCES FOR SECTIONS 1 TO 4

- [1] ALDOR-NOIMAN, S., BROWN, L. D., BUJA, A., ROLKE, W. & STINE, R. A. (2013). The power to see: A new graphical test of normality. *The American Statistician* **67**, 249–260.
- [2] ANDERSON, G. (1994). Simple tests of distributional form. *Journal of Econometrics* **62**, 265–276.
- [3] ARNASTAUSKAITÉ, J., RUGAS, T. & BRAZÉNAS, M. (2021). An exhaustive power comparison of normality tests. *Mathematics* **9**, 788–808.
- [4] BERK, R. H. & JONES, D. H. (1979). Goodness-of-fit test statistics that dominate the Kolmogorov-Smirnov statistics. *Zeitschrift fur Wahrscheinlichkeitstheorie und verwandte Gebiete* **47**, 47–59.
- [5] BHATTACHARJEE, D. & MUKHOPADHYAY, N. (2013). On sequential point estimation in a uniform distribution with adjusted non-sufficient estimators: a comparative study and real data illustration. *Calcutta Statistical Association Bulletin* **65**, 103–121.
- [6] BICKEL, P. J. & DOKSUM, K. A. (1977). *Mathematical Statistics: Basic Ideas and Selected Topics*. San Francisco: Holden-Day.
- [7] BISSANTZ, N., CLAESKENS, G., HOLZMANN, H. & MUNK, A. (2009). Testing for lack of fit in inverse regression—with applications to biophotonic imaging. *Journal of the Royal Statistical Society: Series B* **71**, 25–48.
- [8] BOERO, G., SMITH, J. & WALLIS, K. F. (2004a). Decompositions of Pearson's chi-squared test. *Journal of Econometrics* **123**, 189–193.
- [9] BOERO, G., SMITH, J. & WALLIS, K. F. (2004b). The sensitivity of chi-squared goodness-of-fit tests to the partitioning of data. *Econometric Reviews* **23**, 341–370.
- [10] BOGDAN, M. (1995). Data driven version of Pearson's chi-square test for uniformity. *Journal of Statistical Computation and Simulation* **52**, 217–237.
- [11] ĆMIEL, B., INGLOT, T. & LEDWINA, T. (2020). Intermediate efficiency of some weighted goodness-of-fit statistics. *Journal of Nonparametric Statistics* **32**, 667–703.
- [12] CSÖRGÖ, S. (2003). Weighted correlation tests for location-scale families. *Mathematical and Computer Modeling* **38**, 753–762.
- [13] DEL BARRO, E., CUESTA-ALBERTOS, J., MATRAN, C. & RODRIGUEZ, J. (1999). Tests of goodness of fit based on L_2 -Wasserstein distance. *Annals of Statistics* **27**, 1230–1239.
- [14] DUCHARME, G. R. & FONTEZ, B. (1999). A smooth test of goodness-of-fit for growth curves and monotonic nonlinear regression models. *Biometrics* **60**, 977–986.
- [15] DUCHARME, G. R. & LAFAYE DE MICHEAUX, P. (2004). A goodness-of-fit tests for normality for the innovations in ARMA models. *Journal of Time Series Analysis* **25**, 373–395.
- [16] DUCHARME, G. R. & LAFAYE DE MICHEAUX, P. (2020). A goodness-of-fit test for elliptical distributions with diagnostic capabilities. *Journal of Multivariate Analysis* **178**, 104602.
- [17] DURBIN, J. (1973). Weak convergence of the sample distribution function when parameters are estimated. *Annals of Statistics* **1**, 279–290.
- [18] ESCANCIANO, J. C. & LOBATO, I.N. (2009). An automatic Portmanteau test for serial correlation. *Journal of Econometrics* **151**, 140–149.
- [19] GAN, F. F. & KOEHLER, K. T. (1990). Goodness-of-fit test based on P-P probability plots. *Technometrics* **32**, 289–303.
- [20] GAN, F. F., KOEHLER, K. T. & THOMPSON, J. C. (1991). Probability plots and distribution curves for assessing the fit of probability models. *The American Statistician* **45**, 14–21.
- [21] HANDCOCK, M. S. & MORRIS, M. (1999). *Relative Distribution Methods in the Social Sciences*. Springer: New York.
- [22] HOLMGREN, E. B. (1995). The P-P plot as a method for comparing treatment effects. *Journal of the American Statistical Association* **90**, 360–365.
- [23] KALLENBERG, W. C. M. & LEDWINA, T. (1997). Data driven smooth tests when the hypothesis is composite. *Journal of the American Statistical Association* **92**, 1094–1104.
- [24] INGLOT, T. & LEDWINA, T. (2006). Data driven score tests for a homoscedastic linear regression model: asymptotic results. *Probability and Mathematical Statistics* **26.1**, 41–61.
- [25] INGLOT, T. & JANIC-WRÓBLEWSKA, A. (2003). Data driven chi-square test for uniformity with unequal cells. *Journal of Statistical Computation and Simulation* **73**, 545–561.

- [26] JANIC, A. & LEDWINA, T. (2009). Data driven smooth tests for a location-scale family revisited. *Journal of Statistical Theory and Practice. Special Issue: Modern Goodness of Fit Methods* **3**, 645–664.
- [27] KENDALL, M. G. & BUCKLAND, W. R. (1957). *A Dictionary of Statistical Terms*. Oliver and Boyd: London.
- [28] LEDWINA, T. (1994). Data driven version of Neyman's smooth test of fit. *Journal of the American Statistical Association* **89**, 1000–1005.
- [29] LEDWINA, T. & WYŁUPEK, G. (2012a). Nonparametric tests for first order stochastic dominance. *Test* **21**, 730–756.
- [30] LEDWINA, T. & WYŁUPEK, G. (2012b). Two-sample test for one-sided alternatives. *Scandinavian Journal of Statistics* **39**, 358–381.
- [31] LEDWINA, T. & WYŁUPEK, G. (2015). Detection of non-Gaussianity. *Journal of Statistical Computation and Simulation* **85**, 3480–3497.
- [32] NEYMAN, J. (1937). 'Smooth' test for goodness of fit. *Skandinavisk Aktuarietidskrift* **20**, 149–199.
- [33] PARZEN, E. (2004). Quantile probability and statistical data modelling. *Statistical Science* **19**, 652–662.
- [34] PEÑA, E. A. (2003). Classes of fixed-order and adaptive smooth goodness-of-fit tests with discrete right-censored data. In *Mathematical and Statistical Methods in Reliability*. Series on Quality, Reliability and Engineering Statistics, eds B. Lindqvist and K. Doksum, 485–501.
- [35] ROLKE, W. & GONGORA, C. G. (2021). A chi-square goodness-of-fit test for continuous distributions against a known alternative. *Computational Statistics* **36**, 1885–1900.
- [36] ROSENKRANTZ, W. A. (2000). Confidence bands for quantile functions: a parametric and graphic alternative for testing goodness of fit. *The American Statistician* **54**, 185–190.
- [37] THAS, O. (2001). *Nonparametrical Tests Based on Sample Space Partitions*. Ph.D. thesis, Ghent University.
- [38] THAS, O. (2010). *Comparing Distributions*. Springer: New York.
- [39] THAS, O., RAYNER, J. C. W. & DE NEVE, J. (2015). A generalised smooth tests of goodness of fit utilising L-moments. *Australian and New Zealand Journal of Statistics* **57**, 481–499.
- [40] VOINOV, V. (2010). A decomposition of Pearson-Fisher and Dzaparidze-Nikulin statistics and some ideas for a more powerful test construction. *Communications in Statistics - Theory and Methods* **39**, 667–677.
- [41] WANG, L. & QU, A. (2009). Consistent model selection and data driven smooth tests for longitudinal data in the estimating equation approach. *Journal of the Royal Statistical Society: Series B* **71**, 177–190.

APPENDIX A. REAL DATA EXAMPLES

In this first appendix, we work out six examples to show the useful insights that can be derived using the tools of the paper. Regarding the computation of the acceptance regions, we take inspiration from the example in Section 3.5 and globally consider the tails of the distribution as defined by the first and last deciles, to which we may add a central region more specific to the data.

A.1. The wave record data revisited. We present a more detailed discussion of the analysis of the wave record data presented in Section 3.5. First, to better appreciate the structure of the data, Figure A.1.1 presents the B plot associated with the denser partition $S(n) = 6$. This figure shows that the overall shape of the B plot is retained, while evidences of departure in the tails are better manifested. The question arises whether the conclusions regarding sets of bars hold for this new B plot. We have recomputed $u(66, 0.05, \{1, \dots, 12\}) = 2.27$, $u(66, 0.05, \{116, \dots, 127\}) = 2.57$ and $\ell(66, 0.05, \{58, \dots, 84\}) = -2.43$ and represented the related simultaneous acceptance regions as shaded gray stripes. This shows that increasing $S(n)$ slightly changes the bounds but that the observations of Section 3.5 remain unchanged.

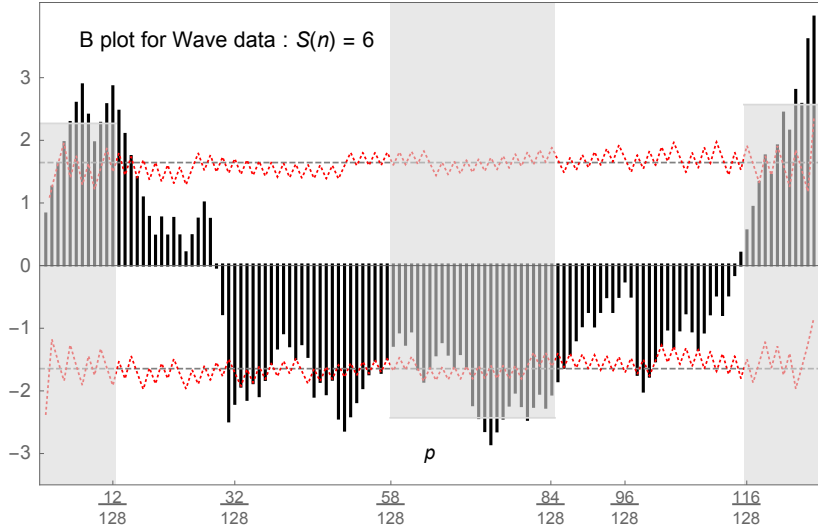


FIGURE A.1.1. B plot of $\sqrt{n} \widehat{CC}(p_{6,j}; \tilde{\beta})$, with $j \in \{1, \dots, 127\}$, for the wave records data ($n = 66$) in Bickel & Doksum (1997). The dashed gray lines are located at ± 1.645 to identify the individual bars where some dissonance with \mathbb{H} : *Gaussianity* occurs at one-sided level 5%. The shaded gray stripes are the simultaneous 5% one-sided acceptance regions for subsets of bars $\{1, \dots, 12\}$, $\{58, \dots, 84\}$ and $\{116, \dots, 127\}$. The dotted red lines are the one-sided (upper and lower) 5% acceptance intervals for individual bars, as obtained by the Monte Carlo method.

By construction, the simultaneous acceptance regions are accurate up to the number of Monte Carlo replications, taken here as 100 000. However, one may inquire about the precision of the asymptotic ± 1.645 individual bounds. In Figure A.1.1 we added (the dotted red lines) the bounds obtained, again from 100 000

Monte Carlo replications. For finite samples, the $\sqrt{n} \widehat{CC}(p_{s,j}; \tilde{\beta})$ have a discrete distribution. But interestingly, even with the small sample considered here ($n = 66$), the asymptotic 5% bounds are sufficiently close to the exact values to be useful throughout the range $p \in (0, 1)$, except perhaps near the outmost boundaries.

Note that a B plot can also provide useful information regarding which test statistic could be more profitably applied to assess overall compatibility between the data and the model. For example, the above analysis exhibits substantial disagreements between the data and the model in the tails. Now, much evidence (see Milbrodt & Strasser, 1990; Ćmiel et al., 2020; Inglot, 2020 and references therein) have been unearthed showing that in such circumstances, the classical Kolmogorov-Smirnov (KS) test is weak: for the wave data we get a p -value of 0.06. B plots present weighted distances between an estimated empirical process and the model CDF. This weighting increases the differences appearing in the KS statistic, thus creating a comparable scale over the whole range of p . In particular, test statistic $\mathcal{M}_{127}(\tilde{\beta})$, which can be considered as a weighted variant of the KS statistic, leads to a p -value of 0.004, comparable with AD, SW and BCMR, thus removing the weakness of the classical KS solution. In contrast, in situations where the B plot shows that most of the discrepancies occur in the central range of quantiles, such classical tests can be adequate tools, see Appendix A.4 and A.5.

The above versions of the B plot are expressed as functions of the quantiles p . A variant B plot can be produced that relates more directly to the original data. To this end, set $\tilde{q}_{s,j} = \tilde{q}_{s,j}(p_{s,j}) = \tilde{\beta}_2 \Phi^{-1}(p_{s,j}) + \tilde{\beta}_1$, which represents the estimated $p_{s,j}$ quantile of the null distribution. With this notation, set

$$\begin{aligned} \widehat{CC}(\tilde{q}_{s,j}; \tilde{\beta}) &= \frac{\Phi((\tilde{q}_{s,j} - \tilde{\beta}_1)/\tilde{\beta}_2) - \hat{F}_n(\tilde{q}_{s,j})}{\sigma_{s,j}} \\ &= \frac{p_{s,j} - \hat{F}_n(\tilde{\beta}_2 \Phi^{-1}(p_{s,j}) + \tilde{\beta}_1)}{\sigma_{s,j}}, \end{aligned}$$

where $\hat{F}(\cdot)$ is the ordinary empirical CDF of the sample. Given s , this variant B plot, noted B_q plot, is obtained by plotting the $\widehat{CC}(\tilde{q}_{s,j}; \tilde{\beta})$ against the $\tilde{q}_{s,j}, j = 1, \dots, d(s)$. Figure A.1.2 shows such a graph for the wave data with $S(n) = 5$ and the related acceptance regions. In particular, one can see that the seven data points greater than $\tilde{q}_{5,58} = 6.9$ are more dispersed to the right than expected under the null hypothesis.

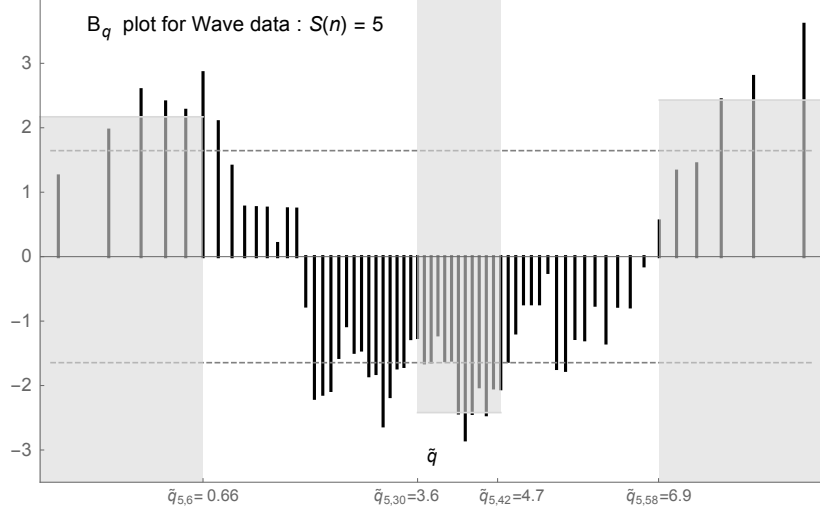


FIGURE A.1.2. B_q plot of the values of $\sqrt{n} \widetilde{CC}(\tilde{q}_{5,j}; \tilde{\beta})$ plotted against the estimated quantiles $\tilde{q}_{5,j}$ with $j \in \{1, \dots, 63\}$, for the wave records data ($n = 66$) in Bickel & Doksum (1997). The dashed gray lines are located at ± 1.645 to identify the individuals bars where some dissonance with \mathbb{H} : *Gaussianity* occurs at one-sided level 5%. The shaded gray stripes are the simultaneous 5% one-sided acceptance regions for subsets of bars $\{1, \dots, 6\}$, $\{30, \dots, 42\}$ and $\{58, \dots, 63\}$.

A.2. The open/closed book examination data. Consider the open book /closed book examination data set in Mardia, Kent & Bibby (1979) pp. 3–4, which gives the marks of a group of $n = 88$ students in Mechanics, Vectors, Algebra, Analysis, and Statistics. The marks in Statistics, Vectors and Analysis were analyzed in Ducharme & Lafaye de Micheaux (2020) who rejected a trivariate multinormal distribution. Here we revisit the marks for Analysis.

For this data set, we have $\tilde{\beta}_1 = \bar{X} = 346.7$ and $\tilde{\beta}_2 = S = 14.84$. We have applied the test based on $\mathcal{P}_{\tilde{Q}(\alpha)}(\tilde{\beta})$ with $S(n) = 4$ and $\alpha = 0.05$. The observed value of \mathcal{T}_n is 5.15, leading to $\tilde{Q}(\alpha) = 31$ with $\mathcal{P}_{\tilde{Q}(\alpha)}(\tilde{\beta}) = 155.12$, to be compared to a 5% critical level of 10.44, interpolated from Table B.3 in Appendix B. Thus we reject the null hypothesis of Gaussianity at the 5% level. The p -values for AD, SW, BCMR are 0.0001 for AD, 0.0001 for SW and 0.001 for BCMR. Thus these tests also reject the Gaussian model at level 5%.

On the B plot of Figure A.2.1, the left tail of the distribution seems heavier than the Gaussian, while the right one could be thinner, thus indicating some asymmetry to the right of the distribution with less mass at the centre. We find, for $S(n) = 4$, $\ell(88, 0.05; \{1, 2, 3\}) = -2.21$, $\ell(88, 0.05; \{29, 30, 31\}) = -1.92$ and, for similar reasons as in Section 3.5, the slightly decentred (to the left) $u(88, 0.05; \{12, \dots, 18\}) = 2.21$. After drawing the related acceptance regions, we can observe that, in all regions, at least one bar goes beyond these acceptance regions, thus more formally supporting the above claims. Note that in Figure A.2.1 and subsequent similar figures in the present appendix, the $\ell(n, \alpha; \{r, \dots, s\})$ and $u(n, \alpha; \{r, \dots, s\})$ for $S(n) = 6$ have been recomputed.

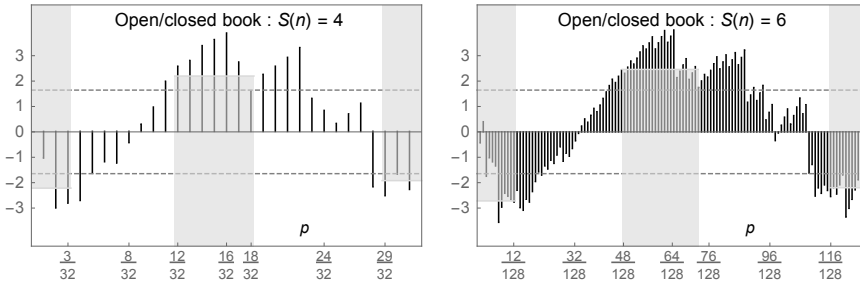


FIGURE A.2.1. B plot of $\sqrt{n} \widehat{CC}(p_{S(n),j}; \tilde{\beta})$ with $S(n) = 4$ and $S(n) = 6$ for the marks in analysis in the open / closed book data ($n = 88$) from Mardia, Kent & Bibby (1979). The dashed gray lines are located at ± 1.645 to identify the bars where dissonance with \mathbb{H} : *Gaussianity* occurs. The shaded gray stripes are the simultaneous 5% one-sided acceptance regions for subsets of bars in the first and last deciles and the slightly decentred central part $p \in (0.37, 0.57)$.

A.3. The cystine data. Consider the cystine content of grade 5 yellow corn. The data ($n = 106$) appear in Gan et al. (1991). In their work they use graphical methods to infer, from the shape of the PP plot, that the Gaussian distribution does not provide an adequate model. However after several attempts, they conclude that no other model they have investigated leads to a clearly better alternative to the Gaussian.

For this data set, we have $\tilde{\beta}_1 = \bar{X} = 0.09$ and $\tilde{\beta}_2 = S = 0.014$. We apply the test based on $\mathcal{P}_{\tilde{Q}(\alpha)}(\tilde{\beta})$ with $S(n) = 4$ and $\alpha = 0.05$. The observed value of \mathcal{T}_n is 4.20, leading to $\tilde{Q}(\alpha) = 31$ with $\mathcal{P}_{\tilde{Q}(\alpha)}(\tilde{\beta}) = 118.52$ to be compared to a 5% critical level of 10.42. Thus the null hypothesis of Gaussianity is rejected at the 5% level. The tests AD, SW and BCMR similarly reject at the 5% level with the p -values for AD : 0.0001, SW : 0.003 and BCMR : 0.005.

As with the example of Section 3.5, a B plot of the $\sqrt{n} \widehat{CC}(p_{S(n),j}; \tilde{\beta})$ for $S(n) = 4$ and $S(n) = 6$, along with the ± 1.645 critical values (see Figure A.3.1) suggests a left tail thinner than the Gaussian and a right tail more consonant with the Gaussian. For $S(n) = 4$, we get $u(106, 0.05; \{1, 2, 3\}) = 2.12$, confirming the claim about the left tail. For the right tail, we find $u(106, 0.05; \{29, 30, 31\}) = 2.05$ and no discrepancy seems to occur there. As for the central part, we consider the quantiles in the wide range $0.33 \approx 11/32 \leq p \leq 21/32 \approx 0.66$ and compute $\ell(106, 0.05; \{11, \dots, 21\}) = -2.40$. The data seems indeed more abundant in this region.

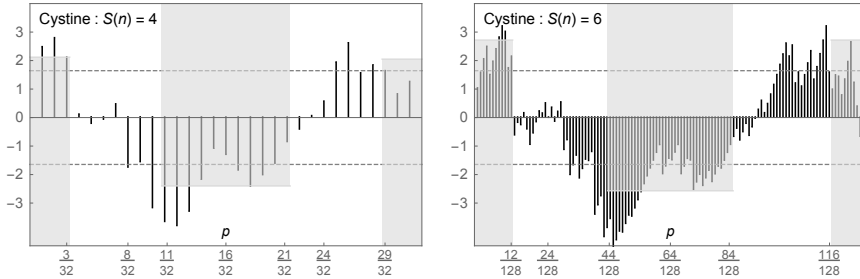


FIGURE A.3.1. B plot of the values of $\sqrt{n} \widehat{CC}(p_{S(n),j}; \tilde{\beta})$ with $S(n) = 4$ and $S(n) = 6$ for the cystine data ($n = 106$) from Gan et al. (1991). The dashed gray lines are located at ± 1.645 to identify the bars where dissonance with \mathbb{H} : *Gaussianity* occurs. The shaded gray stripes are the simultaneous 5% one-sided acceptance regions for subsets of bars in the first and last decile and the middle tier of the distribution.

A.4. The tephra data. We consider the tephra data ($n = 59$) analyzed in Bowman & Azzalini (1997, Sec. 2.5). We apply the transformation into the logistic scale (i.e. $\log(X/(100 - X))$) as done by these authors. For this data, we find $\tilde{\beta}_1 = \bar{X} = 14.56$, $\tilde{\beta}_2 = S = 0.6873$. Here we reverse the order in which our tools were applied in the previous examples and first look at the B plot for this data set, which appears in Figure A.4.1 for $S(n) = 4$ and $S(n) = 6$. A few bars are unexpectedly large under \mathbb{H} , in the slightly decentred region $p \in (16/32, 23/32)$. This is substantiated by computing (for $S(n) = 4$) $u(59, 0.05; \{16, \dots, 23\}) = 2.12$. As stated in Appendix A.1, there is a vast amount of literature providing some hints as to which test is more efficient in some given situations. In particular, when relatively large departures occur near the centre of the data, the classical solutions, e.g. KS, CvM and AD, have been shown to be efficient. For related discussions, see Janssen (2000), Inglot et al. (2000), Ćmiel et al. (2020) along with its supplementary material and references therein. To substantiate this evidence here, we have applied the tests SW and BCMR which do not reject, with p -values for 0.13 of SW and 0.12 for BCMR. The test based on $\mathcal{P}_{\tilde{Q}(\alpha)}(\tilde{\beta})$, with $S(n) = 4$ and using the same constants as previously, yields to an observed value of \mathcal{T}_n of 1.79, leading to $\tilde{Q}(\alpha) = 1$ with $\mathcal{P}_{\tilde{Q}(\alpha)}(\tilde{\beta}) = 3.78$, to be compared to a 5% critical level of 10.47. Thus the null hypothesis of Gaussianity is also not rejected at the 5% level. However, with the KS test, we get a p -value = 0.051 while the AD test yields a p -value = 0.03. This shows that the observation of the B plot can provide some clues as to what test, here the classical solutions, should be subsequently applied to formally detect global departures between the data and the model, while controlling the type I error.

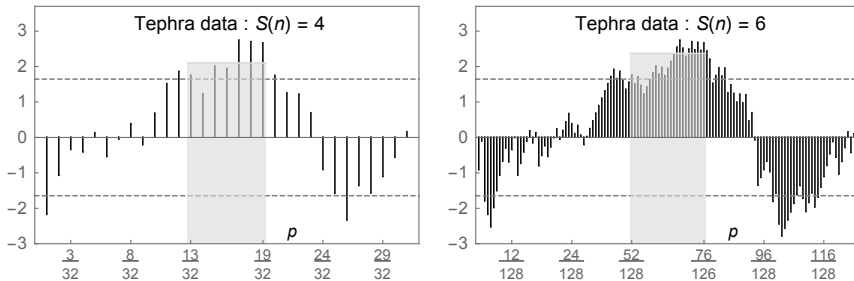


FIGURE A.4.1. B plot of the values of $\sqrt{n} \widehat{CC}(p_{S(n),j}; \tilde{\beta})$, with $S(n) = 4$ and $S(n) = 6$ for the tephra data ($n = 59$) from Bowman & Azzalini (1997). The dashed gray lines are located at ± 1.645 to identify the bars where dissonance with \mathbb{H} : *Gaussianity* occurs. The shaded gray stripe is the simultaneous 5% one-sided acceptance region for bars in the fifth and sixth deciles.

A.5. The PCB data. We consider the PCB data set of Risenbrough ($n = 65$) recalled in Thas (2010, p. 5) and pertaining to the concentration of the chemical PCB (polychlorinated biphenyl) in the yolk lipids of Anacapa (pelican) birds. The data has been thoroughly studied by the author using several graphical methods and one of his conclusions, based on an estimated comparison density, is (Thas, 2010, p. 73) “...the plot suggest weakly that the frequency of PCB concentrations is smaller than expected under the hypothesis of normality”.

For this data, we have $\tilde{\beta}_1 = \bar{X} = 210.0$ and $\tilde{\beta}_2 = S = 72.826$. We again reverse the order in which our tools were applied and look at the B plot for this data set, which appear in Figure A.5.1 and is plotted using both $S(n) = 4$ (with $\ell(65, 0.05; \{16, \dots, 24\}) = -2.26$) and $S(n) = 6$ (with $\ell(65, 0.05; \{64, \dots, 10\}) = -2.49$).

The left half of the distribution appears concordant with the Gaussian hypothesis while the data seems more concentrated toward the centre on the right side. In contrast to previous examples, there seems to be little guidance in the literature suggesting that one of the classical tests for this problem may be preferable in this case. In particular, we get for KS a p -value of 0.057, 0.056 for SW, and 0.057 for AD, all near but above the 0.05 threshold. Note that the BCMR test barely reject Gaussianity with a p -value of 0.049. This is a situation where an adaptive approach such as Thas's (2010) data driven smooth test based on Hermite polynomials, could be useful. Such a test yields a p -value of 0.0325 (p. 120) which leads to rejection of the Gaussian hypothesis. However, the author is unable to derive from the test's components any insight about what may have caused rejection. Our data driven test based on $\mathcal{P}_{\tilde{Q}(\alpha)}(\tilde{\beta})$, with $S(n) = 4$ and using the same constants as previously, yields an observed value of \mathcal{T}_n of 2.64, leading to $\tilde{Q}(\alpha) = 31$ with $\mathcal{P}_{\tilde{Q}(\alpha)}(\tilde{\beta}) = 56.74$, to be compared to a 5% critical level of 10.47. Thus the null hypothesis of Gaussianity is here rejected at the 5% level, a conclusion augmented with the above knowledge derived from the B plot about the discrepancies with the model.

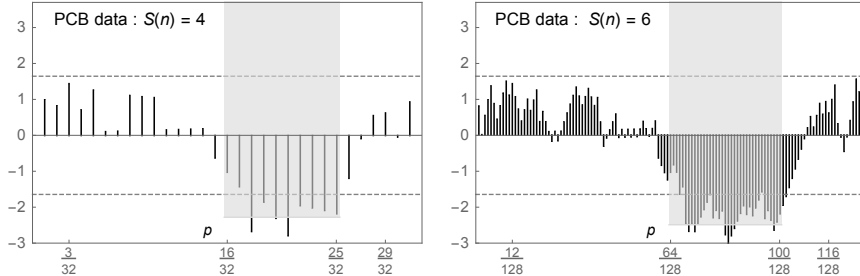


FIGURE A.5.1. B plot of the values of $\sqrt{n} \widehat{CC}(p_{S(n),j}; \tilde{\beta})$, with $S(n) = 4$ and $S(n) = 6$ for the PCB data ($n = 65$). The dashed gray lines are located at ± 1.645 to identify the bars where dissonance with \mathbb{H} : *Gaussianity* occurs. The shaded gray stripes are the simultaneous 5% one-sided acceptance region for bars $\{16, \dots, 25\}$ and $\{64, \dots, 102\}$.

A.6. The smiling baby data set revisited. Here, we revisit the smiling baby data set of Section 2.1, normalized to $[0, 1]$. The B plot of this data for $S(n) = 4$ appears in Panel 2) of Figure 2.1. The B plot associated with $S(n) = 6$ appears in Figure A.6.1. To obtain more precise insights regarding some sets of adjacent bars in the B plot, the variants of $u(n, \alpha, \{r, \dots, s\})$ and $\ell(n, \alpha, \{r, \dots, s\})$ adapted to a simple null hypothesis, with $\widehat{CC}(p_{S(n),j})$ in place of $\widehat{CC}(p_{S(n),j}), \tilde{\beta}$ as explained in Section 3.3, could be computed. However, this is unnecessary here because all individual bars are well within ± 1.645 and no reason emerges to reject uniformity anywhere.

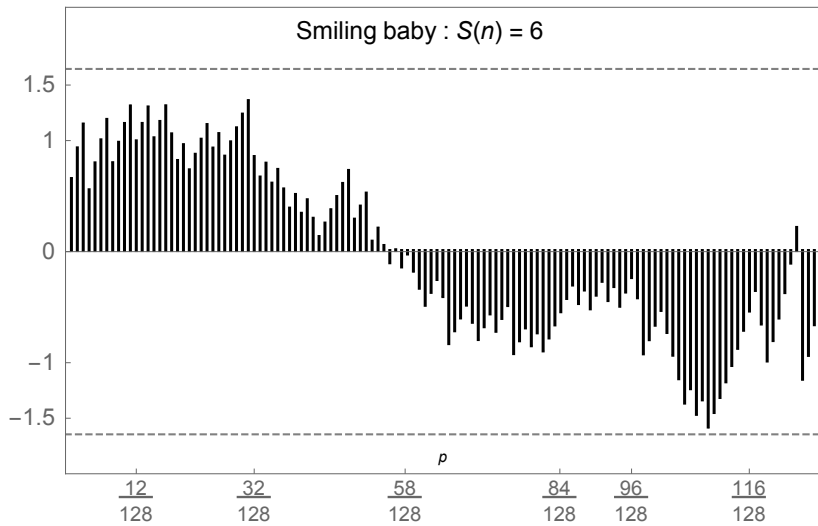


FIGURE A.6.1. B plot of the values of $\sqrt{n} \widehat{CC}(p_{S(n),j})$, with $S(n) = 6$ for the smiling baby data ($n = 55$). The dashed gray lines are located at ± 1.645 to identify the bars where dissonance with $\mathbb{H}_0 : \Phi(\cdot)$ occurs.

To validate this visual assessment, we apply the test based on $\mathcal{P}_{R(\alpha)}$ with $S(n) = 6$ and $\alpha = 0.05$. The observed value of \mathcal{M}_n is 1.59, leading to $R(\alpha) = 1$ with $\mathcal{P}_{R(\alpha)} = 0.16$, to be compared to a 5% critical level of 133.9. Thus we clearly do not reject the null hypothesis of uniformity at the 5% level. This is in agreement with the AD (p -value = 0.63) and BJ (p -value = 0.85) tests.

For these data, we have $\tilde{\beta}_1 = \bar{X} = 0.50$, the median is 0.47 and $\tilde{\beta}_2 = S = 0.26$. From these values, one may wonder whether tests tailored to detect a shift to the left of the median or a smaller dispersion would improve on the above general-purpose GoF procedures, i.e. AD and BJ. The one-sided signed rank test yields a p -value of 0.45 while the one-sided Brown-Forsythe test has a p -value of 0.15. These extra results further support the claim of previous authors (see Bhattacharjee & Mukhopadhyay, 2013) that this data could well be uniformly distributed.

APPENDIX B. DETAILS AND RECOMMENDATIONS ON THE
IMPLEMENTATION OF OUR TOOLS

The practical implementation of our tests requires the choice of $S(n)$ and, depending on whether β is known (the case of \mathbb{H}_0 of Section 2) or must be estimated (the case of $\mathbb{H} : \Phi((x - \beta_1)/\beta_2)$ of Section 3.4), the computation of $a(n, \alpha)$ or $a(n, \alpha; \tilde{\beta})$. In addition, our tests require the values $m(n, \alpha)$ or $t(n, \alpha)$ for the oracles $\mathcal{M}_{D(n)}$ or \mathcal{T}_n as well as the critical values $c(n, \alpha)$ for $\mathcal{P}_{R(\alpha)}$ or $\tilde{c}(n, \alpha)$ for $\mathcal{P}_{\tilde{Q}(\alpha)}(\tilde{\beta})$. In this subsection, we give some details about these values for the cases where $4 \leq S(n) \leq 6$ and for values of n in the range 50, ..., 500, which should cover many situations encountered in practice. Linear interpolations can be used in between entries of the tables.

The values of $a(n, \alpha)$ and $a(n, \alpha; \tilde{\beta})$ are rather stable as functions of n . In particular, one can take $a(n, 0.1) = 2.59$, $a(n, 0.05) = 3.31$ while $a(n, 0.10; \tilde{\beta}) = 2.53$ and $a(n, 0.05; \tilde{\beta}) = 3.18$. Some values of $m(n, \alpha)$ and $t(n, \alpha)$ appear in Tables B.1 and B.2.

n	α	$S(n)$		
		4	5	6
50	10%	2.77	2.79	2.93
	5%	2.89	3.14	3.43
100	10%	2.64	2.79	2.88
	5%	2.92	3.14	3.30
150	10%	2.61	2.78	2.92
	5%	2.96	3.07	3.20
300	10%	2.78	2.97	3.04
	5%	3.04	3.19	3.32
500	10%	2.83	2.93	3.05
	5%	3.04	3.18	3.29

TABLE B.1. Some critical values $m(n, \alpha)$ of $\mathcal{M}_{D(n)}$ in computing $\mathcal{P}_{R(\alpha)}$ for $\mathbb{H}_0 : \Phi(\cdot)$ (simple null hypothesis)

α/n	50	100	50	300	500
0.10	2.15	2.33	2.42	2.57	2.67
0.05	2.52	2.73	2.83	3.00	3.10

TABLE B.2. Some critical values of test statistic \mathcal{T}_n for $\mathbb{H} : \Phi((x - \beta_1)/\beta_2)$ (unknown parameters)

The computation of critical values $c(n, \alpha)$ for $\mathcal{P}_{R(\alpha)}$ is rather straightforward and one can get a good approximation with 25 000 Monte Carlo replications. Such a number is required because this test statistic has a distribution with a discrete component. Table B.3 lists some critical values $\tilde{c}(n, \alpha)$ for $\mathcal{P}_{\tilde{Q}(\alpha)}(\tilde{\beta})$.

n	α	$S(n)$		
		4	5	6
50	10%	7.96	8.43	8.43
	5%	10.48	10.79	10.86
100	10%	8.10	8.29	8.31
	5%	10.43	10.67	10.70
150	10%	8.11	8.32	8.39
	5%	10.33	10.46	10.57
300	10%	7.88	8.07	8.15
	5%	10.01	10.18	10.24
500	10%	7.78	7.94	7.95
	5%	9.71	9.88	9.92

TABLE B.3. Some critical values of $\tilde{c}(n, \alpha)$ for testing $\mathbb{H} : \Phi((x - \beta_1)/\beta_2)$ (unknown parameters) with test statistic $\mathcal{P}_{\tilde{Q}(\alpha)}(\tilde{\beta})$

One must generally be careful when using GoF tests involving an oracle. Such a construction creates a null distribution which is a complex mixture of two components: one when the oracle accepts and another one when it rejects. Regarding statistic $\mathcal{P}_{R(\alpha)}$, this mixture distribution is steep enough so that no difficulty occurs in computing its α -th critical values in the range of conditions we have investigated. However, the null CDF of the counterpart $\mathcal{P}_{\tilde{R}(\alpha)}(\tilde{\beta})$ of $\mathcal{P}_{R(\alpha)}$ is approximately $1 - \alpha$ for a large set of values. This creates instability in computing its α -th critical value, which must be resolved by using over two million MC replications, a serious defect of the procedure. The use here of $\mathcal{P}_{\tilde{Q}(\alpha)}(\tilde{\beta})$, with the penalty $A(1.5; \tilde{\beta})$, slightly less than the Akaike $A(2; \tilde{\beta})$, provides a null distribution where the required critical values are easier to approximate : if necessary, these can be obtained with as little as 25 000 replications for $\alpha = 0.10$ and 0.05 .

With a simple null hypothesis as in Section 2, the power of the oracle $\mathcal{M}_{D(n)}$ increases with $S(n)$ and this in turn affects favourably the power of $\mathcal{P}_{R(\alpha)}$. As a consequence, we recommend using a large value, e.g. $S(n) = 6$, as in the simulations of Section 2.5 and the smiling baby data of Appendix A.6. However, in the context of a composite null hypothesis, the oracle BCMR is not affected by this choice, and this reflects on the powers of $\mathcal{P}_{\tilde{Q}(\alpha)}(\tilde{\beta})$ which are rather stable as a function of $S(n)$. Hence a small value can be used for the GoF test and here we have taken $S(n) = 4$. However, to extract useful insight from the B plot, we recommend first computing the simultaneous acceptance regions with $S(n) = 4$ and, if necessary, use $S(n) = 6$ to get a richer picture of the CC, as we have done in the examples of appendices A.1 to A.6.

APPENDIX C. THE SIMULATION EXPERIMENT FOR A COMPOSITE GAUSSIAN NULL HYPOTHESIS AND RELATED COMMENTS

In this section, we describe the setting and results of the simulation experiment discussed in Section 3.3. Note beforehand that all computations and simulations in the present paper, both in the previous sections and the present appendices, were performed using the Mathematica language (Wolfram Research, Inc., Mathematica, Version 12.1, Champaign, IL, 2020) and the random number generators in the program.

We recall that the null hypothesis is the composite $\mathbb{H} : F(x) = \Phi((x - \beta_1)/\beta_2)$, i.e. we consider testing GoF to the Gaussian distribution. We estimate β by the MLE $\tilde{\beta} = (\bar{X}, S^2)$, so that $\beta_1(F), \beta_2^2(F)$ are the mean and variance of $F(\cdot)$.

The alternatives were selected from some extensive simulation studies and chosen with care to cover a fair range of shapes (see Figure C.1) of $CC(\cdot; \beta(F))$ while embedding, either exactly or approximately, the Gaussian distribution. They are:

- $\mathbb{A}_1(\theta)$, the Tukey distributions with quantile function $\theta^{-1}(q^\theta - (1 - q)^\theta)$ if $\theta \neq 0$ and $\log(q/(1 - q))$ when $\theta = 0$; these are symmetric about 0 unimodal distributions having support $[-1/\theta, 1/\theta]$, if $\theta > 0$ and \mathbb{R} otherwise; $\mathbb{A}_1(0.14)$ is close to a $N(0, 2.142)$, see Pearson et al. (1977);
- $\mathbb{A}_2(\theta)$, normal distributions perturbed by cosine functions with densities $\phi(x)[1 + \theta \cos(4\pi \Phi(x))]$, $\theta \in [0, 1]$ on \mathbb{R} which for $\theta > 0.3$ are visually clearly trimodal, see Inglot et al. (1990); the case $\theta = 0$ yields the $N(0, 1)$;
- $\mathbb{A}_3(\theta) = \mathbb{A}_3^0(\theta)$, the two-piece normal distributions of Section 2.5; these asymmetric distributions have a left tail proportional to a Gaussian, a fat right tail when $\theta > 1$ and a short one otherwise (see Experiment C_2 in Boero et al. 2004; for some history about this distribution, see Wallis, 2014);
- $\mathbb{A}_4(\theta) = \mathbb{A}_4^0(\theta)$, the Fan local model defined in Section 2.5; these densities are asymmetric, bimodal and their tails coincide with those of the $N(0, 1)$ which is $\mathbb{A}_4(0)$ (see Example 5 in Fan, 1996);
- $\mathbb{A}_5(\theta) = \mathbb{A}_5^0(\theta)$, the normal contamination model defined in Section 2.5; the case $\theta = 0$ yields the $N(0, 1)$; see Pearson et al. (1977);
- $\mathbb{A}_6(\theta) = \mathbb{A}_6^0(\theta)$, Anderson's skewed distribution of Section 2.5 the case $\theta = 0$ yields the $N(0, 1)$ (see Experiment C_3 in Boero et al., 2004);
- $\mathbb{A}_7(\theta) = \mathbb{A}_7^0(\theta)$, the Mason & Schuenemeyer (1983) symmetric about zero distribution with CDF $H(\Phi(x), 0.15, \theta)$; the case $\theta = 0$ yields the $N(0, 1)$ (see Ćmiel et al., 2020);
- $\mathbb{A}_8(\theta)$, Johnson's SU distributions, with $X = \sinh(Z/\theta)$, $\theta > 0$ and $Z \sim N(0, 1)$, yielding symmetric about zero and unimodal densities; $\mathbb{A}_8(3.5)$ is approximately $N(0, 0.22)$, see Pearson et al. (1977);
- $\mathbb{A}_9(\theta) = \mathbb{A}_9^0(\theta)$, the Lehmann contamination models from Section 2.5, a contamination model skewed to the left with $\mathbb{A}_9(0) = N(0, 1)$ (see Ćmiel et al., 2020).

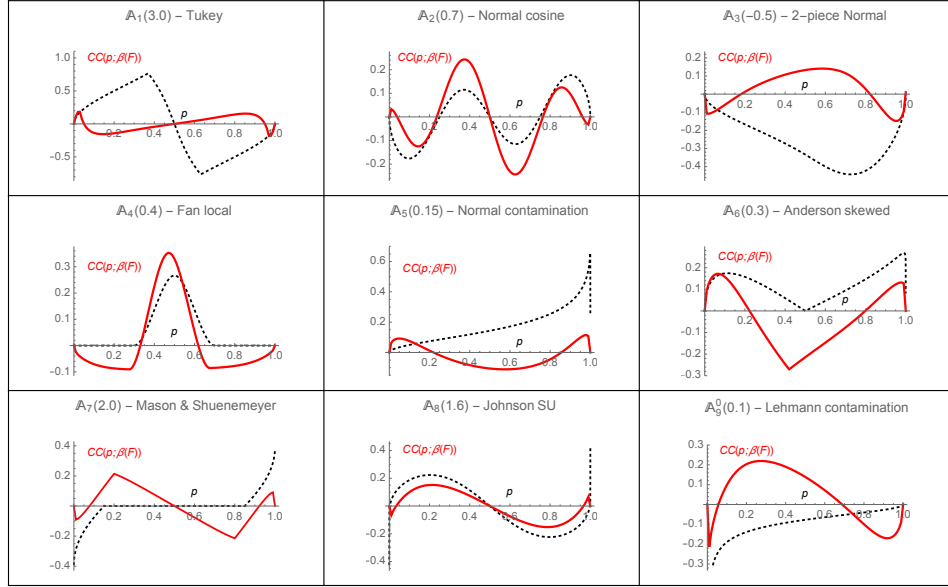


FIGURE C.1. $CC(\cdot; \beta(F))$, $p \in (10^{-5}, 1 - 10^{-5})$ (solid red) for the alternative distributions in Table C.2 for testing the composite null hypothesis $\Phi((x - \beta_1)/\beta_2)$ with (β_1, β_2) unknown. The black dotted curve represents $CC(\cdot)$ of (2.2) corresponding to the simple null model $\Phi((x - \beta_1)/\beta_2)$ with (β_1, β_2) known.

Additionally, note that alternative $A_8^0(\theta)$ in the simulation of Section 2.5 has been extensively used in Experiment D_2 of Boero et al. (2004).

As competitors to $\mathcal{P}_{\tilde{Q}(\alpha)}(\tilde{\beta})$, we have considered the following tests:

- the Anderson-Darling (AD) test adjusted for unknown parameters;
- the Shapiro-Wilks (SW) test;
- the del Barrio et al. (1999) test BCMR.

Taking $\alpha = 0.05$ and $n = 100$, we have investigated $\mathcal{P}_{\tilde{Q}(\alpha)}(\tilde{\beta})$ with the del Barrio et al. (1999) BCMR oracle test using $S(n) = 4$; this yields $a(n, 0.05; \tilde{\beta}) = 3.18$, see Appendix B. The power functions for the nine alternatives were simulated in their θ range for each of the tests $\mathcal{M}_{D(n)}(\tilde{\beta})$ of (3.7) with $D(n) = 31$ and $D(n) = 127$, AD, SW, BCMR and $\mathcal{P}_{\tilde{Q}(\alpha)}(\tilde{\beta})$. The 5% critical value for each test was obtained from 100 000 replications under the null distribution, while the powers were computed from 10 000 Monte Carlo runs. As in Section 2.5, we extracted from each power curve one representative value of θ which provided interesting powers. As a result of these choices, the obtained powers give a comprehensive view of the comparative behaviour of the above tests in a wide range of situations. The results are reported in Table C.2 along the selected value of θ and roughly sorted from thin to fat-tailed. As can be seen, none of the other tests dominates $\mathcal{P}_{\tilde{Q}(\alpha)}(\tilde{\beta})$, which emerges as a good competitor over our range of alternatives.

Alternative	$\mathcal{M}_{31}(\tilde{\beta})$	$\mathcal{M}_{127}(\tilde{\beta})$	AD	SW	BCMR	$\mathcal{P}_{\tilde{Q}(\alpha)}(\tilde{\beta})$
$\mathbb{A}_1(3.0)$	42	38	47	74	70	68
$\mathbb{A}_2(0.7)$	64	60	75	40	41	57
$\mathbb{A}_3(-0.5)$	27	29	43	46	47	45
$\mathbb{A}_4(0.4)$	82	80	78	43	45	65
$\mathbb{A}_5(0.15)$	17	21	28	29	30	28
$\mathbb{A}_6(0.3)$	58	58	73	68	70	69
$\mathbb{A}_7(2.0)$	47	44	56	47	51	56
$\mathbb{A}_8(1.6)$	34	34	47	55	58	53
$\mathbb{A}_9(0.1)$	53	55	68	80	82	75

TABLE C.2. Powers ($n = 100$, $\alpha = 0.05$) of $\mathcal{M}_{D(n)}(\tilde{\beta})$ of (3.7) with $D(n) = 31$ and $D(n) = 127$, the Anderson-Darling (AD), the Shapiro-Wilks (SW), the oracle BCMR and our $\mathcal{P}_{\tilde{Q}(\alpha)}(\tilde{\beta})$ tests for $\mathbb{H}: \Phi((x - \beta_1)/\beta_2)$ with (β_1, β_2) unknown, against a balanced set of alternatives.

In many simulation studies about the empirical power of GoF tests, the alternatives are taken among broad categories such as symmetric, asymmetric, etc. (see Arnastauskaité et al., 2021), often building up on previous simulations by adding some new “interesting” alternatives. In addition, in summarizing their results, many authors base their final recommendations on some averaging of the obtained powers over the alternatives investigated. However, such categories are mostly related to shape of densities, which may not be well adapted to departures related to other characteristics that some GoF tests can detect with greater power than density differences. Thus such averaging can introduce bias in these recommendations.

These recommendations are often of the form “*this test is good at detecting such type of departures*”, with in many cases departures pertaining to asymmetry and large or short tails. However, at the beginning of the modelling process, a user has often limited knowledge about the plausible alternatives to the null model. Hence such recommendations are of little help in choosing a GoF test appropriate to his problem and this will often lead to the use of a *popular* test. This is not good science. Here, examination of the B plot allows acquiring such knowledge and decide whether one can use with some confidence a classical solution or would be better off going through the trouble of considering a much more computationally expensive data driven test, notably the ones of the present work.

The tests of the present paper are based on $CC(\cdot)$, which are aggregated Fourier coefficients (FC) of the respective comparison density. For alternatives defined as in Section 3.2 and in the present appendix, a plot of $CC(\cdot)$ can be produced, and given a variety of such plots, they can be scrutinized to eliminate alternatives with similar shape. Moreover, others can be consciously sought to add diversity in any desired way. Because the magnitude of the FC has a direct relationship with the behaviour of our tests, this helps in producing a less bias appreciation of the comparative power of our proposal.

Power comparisons between the case where $F_0(\cdot; \beta)$ is fully specified and those where β is estimated seldom appear in the literature. Here, in addition to our concern regarding well-balanced set of alternatives, we have made the deliberate choice of selecting three alternatives in common in Tables 1 and C.2, namely the Fan local alternative (\mathbb{A}_4^0 and \mathbb{A}_4), the normal contamination (\mathbb{A}_5^0 and \mathbb{A}_5) and the Lehmann contamination (\mathbb{A}_9^0 and \mathbb{A}_9). This was done to explore the difficulties in going from a simple to a composite null model. It is interesting to see the strong impact the estimation process has on the $CC(\cdot)$. Basically, the expression for $CC(\cdot)$ is modified from (2.2) to (3.3) in which the denominator is different while additionally, in (3.3), $\beta(F)$ plays a role. In all three cases, the forms of $CC(\cdot)$ are rather different (see Figure 2.2 or Figure C.1), and this affects the powers in a way that is difficult to predict. Also, it should be stated that large differences in the forms of the CC curves are sometimes almost imperceptible at the level of densities. This is particularly clear for the Fan alternative ($\mathbb{A}_4^0(0.4)$ and $\mathbb{A}_4(0.4)$). Finally note that, going from the simple null hypothesis to a composite one, the selection rule had to be adapted in an intricate way to preserve the good properties of our procedures. Hence, it can be concluded that the case of unknown parameters is a problem whose complexity is of an order of magnitude above the fully specified case.

APPENDIX D. PROOFS

D.1. Proof of Proposition 1. Note that $\hat{F}_n(F_0^{-1}(p_{s,j})) = n^{-1} \sum_{i=1}^n I(F_0(X_i) \leq p_{s,j})$ where $F_0(X_i)$ are i.i.d. $U(0, 1)$ under \mathbb{H}_0 . Let $\alpha_n(t)$, $t \in [0, 1]$, denote the uniform empirical process. Then it holds that

$$\mathcal{M}_{D(n)} = \max_{1 \leq j \leq D(n)} \frac{|\alpha_n(p_{S(n),j})|}{\sqrt{p_{S(n),j}(1 - p_{S(n),j})}}.$$

Because $D(n) = o(n^{2\delta})$, $\delta \in (0, 1/2)$, for sufficiently large n we get $p_{S(n),1} \geq \epsilon_n = [\log n]^3/n$. Moreover, for the quantity

$$\sup_{\epsilon_n \leq t \leq 1 - \epsilon_n} \frac{|\alpha_n(t)|}{\sqrt{t(1 - t)}},$$

the Darling-Erdős theorem holds, see Jaeschke (1979). This implies that

$$(D.1) \quad \mathcal{M}_{D(n)} = O_P(\sqrt{\log \log n}).$$

Let $c(n, \alpha)$ denote the α -th critical value of $\mathcal{P}_{R(\alpha)}$. On the set $\{\mathcal{M}_{D(n)} > m(n, \alpha)\}$, the value of $\mathcal{P}_{R(\alpha)}$ is equal to $\mathcal{P}_{D(n)}$. Moreover, it holds that

$$\begin{aligned} \text{pr}(\mathcal{P}_{R(\alpha)} \geq c(n, \alpha)) &= \text{pr}(\mathcal{P}_{R(\alpha)} \geq c(n, \alpha) \mid \mathcal{M}_{D(n)} \leq m(n, \alpha)) \\ &\quad \times \text{pr}(\mathcal{M}_{D(n)} \leq m(n, \alpha)) + \text{pr}(\mathcal{P}_{D(n)} \geq c(n, \alpha)) \\ &\quad - \text{pr}(\mathcal{P}_{D(n)} \geq c(n, \alpha), \mathcal{M}_{D(n)} \leq m(n, \alpha)). \end{aligned}$$

Hence, it is enough to show that, under $F(\cdot)$, the test rejecting for large values of $\mathcal{M}_{D(n)}$ is consistent and $\text{pr}(\mathcal{P}_{D(n)} \geq c(n, \alpha)) \rightarrow 1$ as $n \rightarrow \infty$.

We start by showing that, under $F(\cdot)$, the test rejecting for large values of $\mathcal{M}_{D(n)}$ is consistent. By (D.1), $m(n, \alpha)$ cannot grow faster than

$O(\sqrt{\log \log n})$. On the other hand, using the definition of (s_0, j_0) , we have for n large enough

$$\begin{aligned}
 (D.2) \quad \text{pr}(\mathcal{M}_{D(n)} > m(n, \alpha)) &= \text{pr}\left(\max_{1 \leq j \leq D(n)} |\sqrt{n}\hat{\gamma}_j(p_{s,j})| > m(n, \alpha)\right) \\
 &\geq \text{pr}(|\sqrt{n}\hat{\gamma}_{j_0}(p_{s_0,j_0})| > m(n, \alpha)) \\
 &= \text{pr}\left(|\sqrt{n}\gamma_{j_0}(p_{s_0,j_0}) - V_n| > m(n, \alpha)\right),
 \end{aligned}$$

where

$$V_n = \frac{\sqrt{n}[\hat{F}_n(F_0^{-1}(p_{s_0,j_0})) - F(F_0^{-1}(p_{s_0,j_0}))]}{\sqrt{p_{s_0,j_0}(1 - p_{s_0,j_0})}},$$

while $\gamma_{j_0}(p_{s_0,j_0}) = \gamma_{s_0,j_0}$ is defined in (2.6). The numerator in the formula for V_n is $O_P(1)$ while the denominator's impact onto V_n is at most of the order $(D(n))^{-1/2}$. Due to the assumption on $D(n)$, the term V_n is $o_P(n^\delta)$, $\delta \in (0, 1/2)$. Hence, in view of (D.2) and the range of $m(n, \alpha)$, we conclude that under $F(\cdot)$, $\text{pr}(\mathcal{M}_{D(n)} \geq m(n, \alpha)) \rightarrow 1$.

Now we show convergence of $\text{pr}(\mathcal{P}_{D(n)} \geq c(n, \alpha))$ to 1. Because $\mathcal{P}_{R(\alpha)} \leq \mathcal{P}_{D(n)} \leq D(n) \times O_P(\log \log n)$, then $c(n, \alpha) = o(n^{2\delta} \times \log \log n)$. Similarly as in the case of $\mathcal{M}_{D(n)}$, we can write

$$\begin{aligned}
 \text{pr}(\mathcal{P}_{D(n)} \geq c(n, \alpha)) &\geq \text{pr}(|\sqrt{n}\hat{\gamma}_{j_0}(p_{s_0,j_0})| \geq \sqrt{c(n, \alpha)}) \\
 &= \text{pr}(|\sqrt{n}\gamma_{j_0}(p_{s_0,j_0}) - V_n| \geq \sqrt{c(n, \alpha)}).
 \end{aligned}$$

Taking into account the rate of growth of $c(n, \alpha)$, the same argument as above finishes the proof. \square

D.2. Proof of Proposition 2. We start by reducing the consistency problem. Let $\tilde{c}(n, \alpha)$ denote the α -th critical value of $\mathcal{P}_{\tilde{Q}(\alpha)}(\tilde{\beta})$. In the sequel, all probabilities are computed under $F(\cdot)$. Then,

$$\begin{aligned}
 \text{pr}(\mathcal{P}_{\tilde{Q}(\alpha)}(\tilde{\beta}) \geq \tilde{c}(n, \alpha)) &= \text{pr}(\mathcal{P}_{\tilde{Q}(\alpha)}(\tilde{\beta}) \geq \tilde{c}(n, \alpha) \mid \mathcal{T}_n \leq t(n, \alpha)) \\
 &\quad \times \text{pr}(\mathcal{T}_n \leq t(n, \alpha)) \\
 &\quad + \text{pr}(\mathcal{P}_{\tilde{Q}(\alpha)}(\tilde{\beta}) \geq \tilde{c}(n, \alpha) \mid \mathcal{T}_n > t(n, \alpha)) \\
 &\quad \times \text{pr}(\mathcal{T}_n > t(n, \alpha)).
 \end{aligned}$$

From pp.1-2 of the Supplementary Material to Ledwina and Wyłupek (2015), \mathcal{T}_n is consistent under the assumption that $F(\cdot)$ possesses a finite second moment. Hence $\text{pr}(\mathcal{T}_n > t(n, \alpha)) \rightarrow 1$. In view of the above, to prove that $\text{pr}(\mathcal{P}_{\tilde{Q}(\alpha)}(\tilde{\beta}) \geq \tilde{c}(n, \alpha)) \rightarrow 1$, it is enough to show that

$$(D.3) \quad \text{pr}(\mathcal{P}_{\tilde{Q}(\alpha)}(\tilde{\beta}) < \tilde{c}(n, \alpha) \mid \mathcal{T}_n > t(n, \alpha)) \rightarrow 0.$$

The next step is to get the rate of growth of $\tilde{c}(n, \alpha)$. Note that $\mathcal{P}_{\tilde{Q}(\alpha)}(\tilde{\beta}) \leq \mathcal{P}_{D(n)}(\tilde{\beta}) \leq U_n$, where

$$U_n = D(n) \left[n \sup_{0 \leq p \leq 1} |p - \hat{F}_n(\tilde{\beta}_2 F_0^{-1}(p) + \tilde{\beta}_1)|^2 \right] \times \left[\min_{1 \leq j \leq D(n)} \sigma_{S(n),j}^2 \right]^{-1}.$$

Under \mathbb{H} , the first expression in squared brackets is $O_P(1)$ by Durbin's (1973) theorem. The second expression is $O(D(n))$. As a consequence, $U_n = O_P(D^2(n))$ and $\tilde{c}(n, \alpha)$ does not grow faster than $D^2(n)$. Hence, in view of the assumption on $D(n)$, $\tilde{c}(n, \alpha) = o(n)$.

Recall from Section 3.2 the indices s_0 and j_0 such that $CC(p_{s_0, j_0}; \beta(F)) \neq 0$. We have from (3.5), (3.6)

$$\mathcal{P}_{d(s_0)}(\tilde{\beta}) = n \sum_{j=1}^{d(s_0)} \left[\frac{p_{s_0, j} - \hat{F}_n(\tilde{\beta}_2 F_0^{-1}(p_{s_0, j}) + \tilde{\beta}_1)}{\sqrt{p_{s_0, j}(1 - p_{s_0, j})}} \right]^2 = n \sum_{j=1}^{d(s_0)} [\widehat{CC}(p_{s_0, j}; \tilde{\beta})]^2.$$

Now, we show that

$$(D.4) \quad \text{pr}(\sqrt{n}|\widehat{CC}(p_{s_0, j_0}; \tilde{\beta})| \geq \sqrt{\tilde{c}(n, \alpha)}) \rightarrow 1 \text{ as } n \rightarrow \infty.$$

To this end, observe that

$$(D.5) \quad \sqrt{n}[\widehat{CC}(p_{s_0, j_0}; \tilde{\beta})] = \sqrt{n}[CC(p_{s_0, j_0}; \beta(F))] + [W_n^{(1)}(s_0, j_0; \tilde{\beta}) + W_n^{(2)}(s_0, j_0; \tilde{\beta})] \times [\sigma_{s_0, j_0}]^{-1},$$

where

$$(D.6) \quad W_n^{(1)}(s_0, j_0; \tilde{\beta}) = \sqrt{n}[F(\tilde{\beta}_2 F_0^{-1}(p_{s_0, j_0}) + \tilde{\beta}_1) - \hat{F}_n(\tilde{\beta}_2 F_0^{-1}(p_{s_0, j_0}) + \tilde{\beta}_1)],$$

while

$$(D.7) \quad W_n^{(2)}(s_0, j_0; \tilde{\beta}) = \sqrt{n}[F(\beta_2(F)F_0^{-1}(p_{s_0, j_0}) + \beta_1(F)) - F(\tilde{\beta}_2 F_0^{-1}(p_{s_0, j_0}) + \tilde{\beta}_1)].$$

The deterministic term in (D.6) is $O(\sqrt{n})$. The term $W_n^{(1)}(s_0, j_0; \tilde{\beta})$ can be majorized by $\sqrt{n} \sup_{x \in \mathbb{R}} |F(x) - \hat{F}_n(x)|$ and is thus $O_P(1)$. Using the equality $F(x) - F(y) = (x - y)f(z^*)$, where $f(\cdot)$ is the density of $F(\cdot)$ and $\min\{x, y\} \leq z^* \leq \max\{x, y\}$, we see that

$$(D.8) \quad W_n^{(2)}(s_0, j_0; \tilde{\beta}) = \sqrt{n}[(\tilde{\beta}_2 - \beta_2(F))F_0^{-1}(p_{s_0, j_0}) + (\tilde{\beta}_1 - \beta_1(F))]f(Z^*).$$

Under the assumption on the fourth moment of $F(\cdot)$, $\tilde{\beta}_1$ and $\tilde{\beta}_2$ are \sqrt{n} -consistent. By boundedness of $f(\cdot)$, the expression (D.7) is $O_P(1)$. Thus, by the above, $\sqrt{n} \widehat{CC}(p_{s_0, j_0}; \tilde{\beta}) = O_P(\sqrt{n})$. Because $\tilde{c}(n, \alpha) = o(n)$, we get $\mathcal{P}_{d(s_0)}(\tilde{\beta}) \rightarrow \infty$.

Now,

$$(D.9) \quad \begin{aligned} & \text{pr}(\tilde{Q}(\alpha) < d(s_0), \mathcal{T}_n > t(n, \alpha)) \\ & \leq \sum_{s=1}^{s_0-1} \text{pr}(\mathcal{P}_{d(s)}(\tilde{\beta}) - 1.5 \times d(s) \geq \mathcal{P}_{d(s_0)}(\tilde{\beta}) - 1.5 \times d(s_0)). \end{aligned}$$

For $s < s_0$ it holds that $CC(p_{s, j}; \beta(F)) = 0$, $j = 1, \dots, d(s)$. Therefore, by (D.5) to (D.8) applied to such s and related $p_{s, j}$, we have $\mathcal{P}_{d(s)}(\tilde{\beta}) = O_P(1)$. But it was earlier shown that $\mathcal{P}_{d(s_0)}(\tilde{\beta}) \rightarrow \infty$ as $n \rightarrow \infty$. It follows that $\text{pr}(\tilde{Q}(\alpha) < d(s_0)) \rightarrow 0$ on the set $\{\mathcal{T}_n > t(n, \alpha)\}$, as $n \rightarrow \infty$.

Getting back to (D.3), we have

$$(D.10) \quad \begin{aligned} \text{pr}(\mathcal{P}_{\tilde{Q}(\alpha)}(\tilde{\beta}) < \tilde{c}(n, \alpha)) &= \text{pr}(\mathcal{P}_{\tilde{Q}(\alpha)}(\tilde{\beta}) < \tilde{c}(n, \alpha), \tilde{Q}(\alpha) < d(s_0)) \\ &+ \sum_{s=s_0}^{D(n)} \text{pr}(\mathcal{P}_{\tilde{Q}(\alpha)}(\tilde{\beta}) < \tilde{c}(n, \alpha), \tilde{Q}(\alpha) = d(s)). \end{aligned}$$

If $\tilde{Q}(\alpha) \geq d(s_0)$, then $\mathcal{P}_{\tilde{Q}(\alpha)}(\tilde{\beta}) \geq \mathcal{P}_{d(s_0)}(\tilde{\beta})$. Moreover, on the set $\{\mathcal{T}_n > t(n, \alpha)\}$, the first summand in (D.10) is $o(1)$. By the above

$$(D.11) \quad \begin{aligned} \text{pr}(\mathcal{P}_{\tilde{Q}(\alpha)}(\tilde{\beta}) < \tilde{c}(n, \alpha)) &\leq o(1) + D(n) \text{pr}(\mathcal{P}_{d(s_0)}(\tilde{\beta}) < \tilde{c}(n, \alpha)) \\ &\leq o(1) + D(n) \text{pr}(\sqrt{n}|\widehat{CC}(p_{s_0, j_0}; \tilde{\beta})| < \sqrt{\tilde{c}(n, \alpha)}). \end{aligned}$$

This shows that we need to sharpen (D) by studying the rate at which the probability appearing in (D.11) tends to 0. But in view of (D.5) – (D.8) the event $\mathbb{E}_n = \{\sqrt{n}|\widehat{CC}(p_{s_0, j_0}; \tilde{\beta})| < \sqrt{\tilde{c}(n, \alpha)}\}$ reads as

$$(D.12) \quad \mathbb{E}_n = \{\sqrt{n}l_n < W_n^{(1)}(s_0, j_0; \tilde{\beta}) + W_n^{(2)}(s_0, j_0; \tilde{\beta}) < \sqrt{n}u_n\},$$

where

$$\begin{aligned} l_n &= \sigma_{s_0, j_0} \left\{ -\sqrt{n^{-1}\tilde{c}(n, \alpha)} - CC(p_{s_0, j_0}; \beta(F)) \right\}, \\ u_n &= \sigma_{s_0, j_0} \left\{ +\sqrt{n^{-1}\tilde{c}(n, \alpha)} - CC(p_{s_0, j_0}; \beta(F)) \right\}. \end{aligned}$$

Because $\tilde{c}(n, \alpha) = o(n)$, we get $l_n = O(1)$ and $u_n = O(1)$. If $CC(p_{s_0, j_0}; \beta(F)) < 0$, then we can write $\text{pr}(\mathbb{E}_n) \leq \text{pr}(W_n^{(1)}(s_0, j_0; \tilde{\beta}) + W_n^{(2)}(s_0, j_0; \tilde{\beta}) > \sqrt{n}l_n)$. Otherwise, we can consider $\text{pr}(\mathbb{E}_n) \leq \text{pr}(-W_n^{(1)}(s_0, j_0; \tilde{\beta}) + W_n^{(2)}(s_0, j_0; \tilde{\beta}) > \sqrt{n}(-u_n))$. Hence, the triangle inequality, the DKW inequality applied to $W_n^{(1)}(s_0, j_0; \tilde{\beta})$ and Markov's inequality applied to both terms of $W_n^{(2)}(s_0, j_0; \tilde{\beta})$ appearing in (D.8) show that $\text{pr}(\mathbb{E}_n) = O(n^{-1})$. In view of the assumption $D(n) = o(n^{1/2})$ we have $D(n)\text{pr}(\mathbb{E}_n) = o(1)$ and by (D.11), the proof is complete. \square

D.3. Proof of Remark 1. The relations (D.5) – (D.8), expressed in terms of an arbitrary $p \in [\epsilon, 1 - \epsilon]$, imply that

$$\sup_{\epsilon \leq p \leq 1 - \epsilon} \sqrt{n}|\widehat{CC}(p; \tilde{\beta}) - CC(p; \beta(F))| = O_P(1).$$

Hence the statement of Remark 1 follows. \square

REFERENCES FOR APPENDICES

- [1] BHATTACHARJEE, D. & MUKHOPADHYAY, N. (2013). On sequential point estimation in a uniform distribution with adjusted non-sufficient estimators: a comparative study and real data illustration. *Calcutta Statistical Association Bulletin* **65**, 103–121.
- [2] BICKEL, P. J. & DOKSUM, K. A. (1977). *Mathematical Statistics: Basic Ideas and Selected Topics*. San Francisco: Holden-Day.
- [3] BOERO, G., SMITH, J. & WALLIS, K. F. (2004). The sensitivity of chi-squared goodness-of-fit tests to the partitioning of data. *Econometric Reviews* **23**, 341–370.
- [4] BOWMAN, A. W. & AZZALINI, A. (1997). *Applied Smoothing Techniques for Data Analysis*. Clarendon Press: Oxford.

- [5] ĆMIEL, B., INGLOT, T. & LEDWINA, T. (2020). Intermediate efficiency of some weighted goodness-of-fit statistics. *Journal of Nonparametric Statistics* **32**, 667–703.
- [6] DUCHARME, G. R. & LAFAYE DE MICHEAUX, P. (2020). A goodness-of-fit test for elliptical distributions with diagnostic capabilities. *Journal of Multivariate Analysis* **178**, 104602.
- [7] FAN, J. (1996). Test of significance based on wavelet thresholding and Neyman's truncation. *Journal of the American Statistical Association* **91**, 674–688.
- [8] GAN, F. F., KOEHLER, K. T. & THOMPSON, J. C. (1991). Probability plots and distribution curves for assessing the fit of probability models. *The American Statistician* **45**, 14–21.
- [9] INGLOT, T., JURLEWICZ, T. & LEDWINA, T. (1990). On Neyman-type smooth tests of fit. *Statistics* **21**, 549–558.
- [10] INGLOT, T. (2020). Intermediate efficiency of tests under heavy-tailed alternatives. *Probability and Mathematical Statistics* **40**, 331–348.
- [11] INGLOT, T., KALLENBERG, W. C. M. & LEDWINA, T. (2000). Vanishing shortcoming and asymptotic relative efficiency. *Annals of Statistics* **28**, 215–238.
- [12] JAESCHKE, D. (1979). The asymptotic distribution of the supremum of the standardized empirical distribution function on subintervals. *Annals of Statistics* **7**, 108–115.
- [13] JANSSEN, A. (2000). Global power functions of goodness of fit tests. *Annals of Statistics* **28**, 239–253.
- [14] MARDIA, K. V., KENT, J. T. & BIBBY, J. M. (1979). *Multivariate Analysis*. Academic Press: London.
- [15] MASON, D. M. & SCHUENMEYER, J. H. (1983). A modified Kolmogorov-Smirnov test sensitive to tail alternatives. *The Annals of Statistics* **11**, 933–946.
- [16] MILBRODT, H. & STRASSER, H. (1990). On asymptotic power of the two-sided Kolmogorov-Smirnov test. *Journal of Statistical Planning and Inference* **26**, 1–23.
- [17] PEARSON E. S., D'AGOSTINO, R. B. & BOWMAN, K. O. (1977). Tests for departures from normality: comparison of powers. *Biometrika* **64**, 231–246.
- [18] THAS, O. (2010). *Comparing Distributions*. Springer: New York.
- [19] WALLIS, K. F. (2014). The two-piece normal, binormal or double Gaussian distribution: Its origin and rediscoveries. *Statistical Science* **29**, 106–112.
- [20] WOLFRAM RESEARCH, INC. (2020). *Mathematica ,Version 12.1*. Wolfram Research, Inc.: Champaign, Illinois.

IMAG, UNIV MONTPELLIER, CNRS, MONTPELLIER, FRANCE
Email address: gilles.ducharme@umontpellier.fr

INSTITUTE OF MATHEMATICS, POLISH ACADEMY OF SCIENCES, UL. KOPERNIKA 18, 51-617,
 WROCŁAW, POLAND
Email address: ledwina@impan.pl